

1 **The effect of local and regional sources on the isotopic composition of nitrous oxide in the**
2 **tropical free troposphere and tropopause layer**

3

4 Philip Croteau,¹ Elliot L. Atlas,² Sue M. Schauffler,³ Donald R. Blake,⁴ Glenn S. Diskin,⁵
5 Kristie A. Boering^{1,6}

6

7 ¹ University of California, Berkeley, Department of Chemistry, Berkeley, CA 94720, USA

8 ² University of Miami, Division of Marine and Atmospheric Chemistry, Miami, Florida 33149, USA

9 ³ National Center for Atmospheric Research, Atmospheric Chemistry Division, Boulder,
10 Colorado 80307-3000, USA

11 ⁴ University of California, Irvine, Dept. of Chemistry, Irvine, CA 92697-2025, USA

12 ⁵ NASA Langley Research Center, Chemistry and Dynamics Branch, Hampton, VA 23681, USA

13 ⁶ University of California, Berkeley, Department of Earth and Planetary Science, Berkeley, CA
14 94720, USA

15

16 **Submitted to JGR-Atmospheres**

17 **August 31, 2009**

18 **Abstract**

19 Measurements and models of the spatiotemporal variability of surface N₂O mixing ratios and
20 isotopic compositions are increasingly used to constrain the global N₂O budget. However, large
21 variability observed on the small spatial scales of soil chambers and shipboard sampling, which
22 appear to be very sensitive to local environmental conditions, has made extrapolation to the
23 global scale difficult. In this study, we present measurements of the isotopic composition of N₂O
24 ($\delta^{15}\text{N}^{\text{bulk}}$, $\delta^{15}\text{N}^{\alpha}$, $\delta^{15}\text{N}^{\beta}$, and $\delta^{18}\text{O}$) from whole-air samples collected at altitudes of 500m to 19km
25 by the NASA DC-8 and WB-57 aircraft during the Costa Rica Aura Validation Experiment
26 (CRAVE) and the Tropical Composition Cloud and Climate Coupling (TC⁴) campaigns in
27 January-February 2006 and July-August 2007, respectively. The vertical profiles of isotopic
28 composition showed predictable, repeating patterns consistent with the influence of a surface
29 source of N₂O at lower altitudes and the influence of stratospheric photochemistry in the upper
30 Tropical Tropopause Layer and above. Their correlations with marine tracers at lower altitudes
31 are consistent with a predominantly oceanic source, although a soil source cannot be ruled out.
32 Measurements in a combustion plume revealed a strong depletion in ¹⁵N at the central nitrogen
33 atom (i.e., low $\delta^{15}\text{N}^{\alpha}$ values), providing new information on N₂O isotopic compositions from
34 combustion. This new dataset demonstrates that a coherent picture of the isotopic composition of
35 tropospheric N₂O is possible at currently attainable precisions and that its variability from 500m
36 to the lower stratosphere is a useful tool in investigating the sources and distributions of this
37 important greenhouse gas.

41 **1. Introduction**

42 Nitrous oxide, N₂O, is an important greenhouse gas with a tropospheric mixing ratio that
43 has risen from a pre-industrial level of ~270 ppbv to current levels of ~320 ppbv [e.g.,
44 *MacFarling-Meure et al.*, 2006], revealing an imbalance between the N₂O sources and sinks of
45 ~5 TgNyr⁻¹ [*Forster et al.*, 2007]. The magnitudes of the particular processes that contribute to
46 this imbalance (and how these may change as climate changes and as a side-effect of CO₂
47 mitigation strategies) have large uncertainties [e.g., *Forster et al.*, 2007]. Atmospheric N₂O
48 originates predominantly at Earth's surface as a product or byproduct of microbial nitrification
49 and denitrification in water and in both natural and agricultural soils, and is emitted to the
50 atmosphere by air-sea and air-soil exchange. These processes also yield N₂O with oxygen and
51 nitrogen isotopic compositions that depend on the isotopic composition of the N and O reservoirs
52 from which it is produced as well as isotope effects associated with the microbiogeochemistry of
53 N₂O production and consumption. The only major N₂O sink is destruction by photolysis and
54 reaction with O(¹D) in the stratosphere, which enriches the remaining N₂O in the heavy isotopes
55 ¹⁵N and ¹⁸O [e.g., *Kim and Craig*, 1993]. Since the sources and sinks of atmospheric N₂O
56 determine its isotopic composition, isotope measurements can provide additional constraints on
57 the N₂O budget beyond those based on measurements of N₂O mixing ratios alone [e.g., *Kim and*
58 *Craig*, 1993; *Toyoda et al.*, 2002; *Park et al.*, 2004].

59 So far, however, the large variability in N₂O isotopic compositions measured in and
60 above soils [e.g., *Pérez et al.*, 2000, 2001] and the oceans [e.g., *Popp et al.*, 2002; *Toyoda et al.*,
61 2002] has precluded a “bottom up” approach to simultaneously balancing the global N₂O
62 concentration and isotope budgets. Isotopic compositions of emitted N₂O appear to depend
63 sensitively on small-scale variations in many environmental parameters such as soil texture, soil

64 water content, and substrate isotopic composition (e.g., nitrates), as well as the relative amounts
65 of nitrification, denitrification, and consumption. Indeed, apportioning the relative amounts of
66 N₂O from nitrification and denitrification and the amount of N₂O consumption in the soils before
67 emission to the atmosphere is one of the goals of using isotope measurements at the field scale
68 [e.g., *Bol et al.*, 2003; *Pérez et al.*, 2006]; knowledge of how the magnitudes of these processes
69 change with environmental variables could be used to adjust agricultural parameters, such as soil
70 water content during fertilization, in order to mitigate the release of N₂O to the atmosphere and
71 to better predict effective mitigation strategies as mean surface temperatures rise. However, this
72 large variability has also meant that a “bottom up” approach to balancing the regional,
73 hemispheric, and global budgets is unlikely to be sufficiently constrained.

74 A “top-down” approach via inverse modeling of N₂O measurements [*Hirsch et al.*, 2006]
75 has also been underconstrained, at least apart from box model studies of the long-term increase
76 in N₂O concentrations and the concurrent depletion in its heavy isotopes that have been
77 measured in air from firn and ice cores [*Rahn and Wahlen*, 2000; *Sowers et al.*, 2002; *Röckmann*
78 *et al.*, 2005; *Bernard et al.*, 2006]. Due to its long atmospheric lifetime, N₂O (and hence its
79 isotopic composition) has been assumed to be well-mixed and thus expected to show little
80 variation in the troposphere, leaving inverse models underconstrained. Recently, however, time
81 series analyses [*Nevison et al.*, 2005, 2007; *Jiang et al.*, 2007] of nearly continuous high-
82 precision N₂O mixing ratio measurements at the surface have revealed detectable seasonal cycles
83 and interannual variations in N₂O concentrations, and new N₂O isotope measurements on
84 archived air samples from the surface at Cape Grim, Tasmania reveal the same [*Park et al.* 2005,
85 2008], demonstrating that a top-down approach using these datasets could ultimately help
86 constrain the magnitudes of different sources. Further information on the isotopic compositions

87 of N₂O emitted from the oceans and soils and the degree to which they may affect regional and
88 hemispheric N₂O isotopic compositions are greatly needed to proceed, however, as there is a
89 dearth of observations.

90 Here, we report measurements of the ¹⁸O and ¹⁵N isotopic compositions (including site-
91 specific ¹⁵N) of N₂O in whole air samples collected from 500m to the lower stratosphere in the
92 tropics. The N₂O isotope altitude profiles obtained in both January and July in different years
93 show a persistent pattern that our initial analysis suggests reflects the influence of N₂O most
94 likely from the ocean at lower altitudes, transitioning to the influence of stratospheric
95 photochemistry in the TTL and above the tropopause. Although the variations are small, they are
96 detectable at current measurement precisions using continuous-flow Isotope Ratio Mass
97 Spectrometry (cf-IRMS). As such, these measurements, combined with future vertical profiles in
98 different regions and with increased measurement precision, may finally succeed in allowing
99 isotopes to be used in a “top down” approach to constrain the magnitude and distribution of
100 anthropogenic and natural N₂O sources.

101 **2. Methods**

102 Whole air samples were collected from the WB-57 aircraft in January and February 2006
103 during the Costa Rica Aura Validation Experiment (CRAVE) and from the WB-57 and DC-8
104 aircraft in July and August 2007 during Tropical Composition, Cloud and Climate Coupling
105 (TC⁴), both NASA missions based in San Jose, Costa Rica (9.99°N, 84.21°W). The University of
106 Miami (UM) whole air sampler (WAS) [Flocke *et al.* 1999], which flew on the WB-57, included
107 50 1.5-liter electropolished stainless steel canisters equipped with automated metal valves. The
108 evacuated canisters were pressurized to 40 psi using a 4-stage bellows pump in flight. The
109 University of California, Irvine (UCI) whole air sampler [Colman *et al.*, 2001], which flew on

110 the DC-8, used a stainless-steel, grease-free bellows pump to pressurize 2-L stainless steel
111 canisters to 40 psi. The canisters were equipped with stainless steel bellows valves and were
112 evacuated and then filled with ~20 Torr of water vapor prior to the flights. Samples were
113 collected in the planetary boundary layer, the free troposphere, through the TTL, and into the
114 lower stratosphere. Most of the WB-57 samples selected for isotopic analysis (see below) were
115 collected between ~10 and 20 km, and those selected from among the DC-8 samples were
116 collected between ~0.5 and 11.5 km. For reference, the cold-point tropopause was located on
117 average at ~16.5 km during TC⁴ and ~17.5 km during CRAVE. Most of the samples selected for
118 isotopic analysis were collected between ~ 1°S and 10°N, but 25 of the samples were collected
119 between ~20 and 30°N on two similar WB-57 transit flights (one for TC⁴ and one for CRAVE)
120 between Costa Rica and Houston, Texas.

121 After sample collection, the WB-57 and the DC-8 whole air samples were first measured
122 for numerous trace gas mixing ratios at UM and UCI, respectively, by gas chromatography (GC)
123 gas-chromatography-mass spectrometry (GC-MS). For the WB-57 WAS samples, measurements
124 that are relevant for this study are mixing ratios of N₂O, ethane (C₂H₆), propane (C₃H₈), benzene
125 (C₆H₆), and tetrachloroethylene (C₂Cl₄). In particular, N₂O mixing ratio measurements were
126 made using an HP5890 II+ series GC fitted with an electron capture detector (ECD) relative to a
127 314 ppbv N₂O secondary standard of whole air calibrated against a National Institute of
128 Standards and Technology (NIST) reference gas, Standard Reference Material #2608 with an
129 N₂O mixing ratio of 300 nmol/mol ± 1%. The average uncertainty (2σ) for the N₂O mixing ratio
130 data is less than 0.7 ± 1% [Hurst *et al.*, 2002]. Hydrocarbon species were measured by GC with
131 flame ionization detection (GC-FID) with limits of detection (LOD) of about 2 ppt. C₂Cl₄ was
132 measured with GC mass spectrometry (GC-MS) with LOD of better than 0.1 pptv. For the DC-

133 8 samples, measurements that are relevant for this study include mixing ratios of methyl iodide
134 (CH_3I), methyl nitrate (CH_3ONO_2 or “ MeONO_2 ”), and ethyl nitrate ($\text{C}_2\text{H}_5\text{ONO}_2$ or “ EtONO_2 ”),
135 ethyne and benzene. CH_3I , MeONO_2 , and EtONO_2 were measured by GC-ECD with LODs of
136 0.01, 0.02, and 0.02 pptv, respectively. Ethyne and benzene were measured by GC-FID, both
137 with LODs of 3 pptv. Our analyses also included correlations of the N_2O isotope measurements
138 with *in situ* measurements of carbon monoxide (CO) and methane (CH_4) mixing ratios from a
139 tunable diode laser instrument, DACOM [Sachse *et al.*, 1987, 1991]; measurements were made
140 at 1 Hz measurement with 0.1% precision and were averaged over the whole air canister
141 sampling interval to compare with the whole air sample measurements. N_2O mixing ratio
142 measurements sometimes made using the DACOM instrument are not available for these flights.
143 Attempts to retrieve an N_2O mixing ratio from a combination of peak area from the isotope ratio
144 measurements (described below) and the sample pressure at the time of the isotope analyses were
145 not successful due to uncertainties in the precise amount of water vapor in the sample canisters
146 from the ~ 20 -Torr preconditioning noted above and in the absolute total pressure due to the fact
147 that a convection gauge that was not calibrated for wet samples was used as a housekeeping
148 measurement and was not intended to provide an accurate absolute pressure measurement
149 independent of the gaseous composition.

150 After these and other trace gas mixing ratio measurements at UM and UCI, a total of 125
151 samples were selected for isotopic analysis and shipped to the University of California, Berkeley.
152 The isotopic composition of N_2O in the whole air samples was measured at UC Berkeley by
153 continuous-flow isotope ratio mass spectrometry (cf-IRMS) on a Finnigan MAT-252 coupled
154 with preconcentration (PreCon) and gas chromatography (GC) devices – i.e., “PreCon/GC/cf-
155 IRMS.” Prior to the isotope measurements, the CRAVE whole-air samples were archived in 1.5-

156 liter Pyrex flasks; aliquots for the isotope measurements were taken from these archival flasks by
157 expansion into evacuated 100-200mL measurement flasks. The TC⁴ samples were not archived;
158 100 ml aliquots for isotope analysis were taken directly from the sample canisters.

159 N₂O isotopic compositions are reported here as δ -values in “per mil” (‰), which is the
160 part per thousand difference of the isotope ratio of the sample relative to a standard: $\delta =$
161 $1000 \cdot (R/R_{\text{standard}} - 1)$, where $R = {}^{15}\text{N}/{}^{14}\text{N}$ or ${}^{18}\text{O}/{}^{16}\text{O}$ and the subscript ‘standard’ refers to an
162 international reference material, which is air-N₂ for $\delta^{15}\text{N}$ and Vienna Standard Mean Ocean
163 Water (VSMOW) for $\delta^{18}\text{O}$. Two types of nitrogen isotopic compositions are reported: (1)
164 $\delta^{15}\text{N}^{\text{bulk}}$, which is the ${}^{15}\text{N}$ isotope composition averaged over the two nitrogen atom sites in N₂O,
165 and (2) $\delta^{15}\text{N}^{\alpha}$ and $\delta^{15}\text{N}^{\beta}$, which represent the “site-specific” isotopic compositions – i.e., the ${}^{15}\text{N}$
166 isotopic composition at the central nitrogen atom (the “ α ” site) and the ${}^{15}\text{N}$ isotopic composition
167 at the terminal nitrogen atom (the “ β ” site), respectively. Although for several years there had
168 been controversy regarding how to convert $\delta^{15}\text{N}^{\alpha}$ and $\delta^{15}\text{N}^{\beta}$ IRMS measurements onto the
169 international air-N₂ scale [e.g., *Toyoda and Yoshida, 1999; Kaiser et al. 2004; Park et al., 2004;*
170 *Westley et al. 2007*], Griffith *et al.* [2009] recently determined the Site Preference (SP =
171 ${}^{15}\text{R}^{\alpha}/{}^{15}\text{R}^{\beta} - 1$) of tropospheric N₂O using a Fourier Transform infrared spectroscopic technique
172 which is independent of mass spectrometric measurements, yielding values that are in agreement
173 with the Toyoda and Yoshida [1999] air-N₂ scale. Thus, we report $\delta^{15}\text{N}^{\alpha}$ and $\delta^{15}\text{N}^{\beta}$ values on the
174 Toyoda and Yoshida [1999] scale.

175 Since the details of the isotopic measurements have been described elsewhere [*Park et*
176 *al., 2004*], only a brief overview is given here. Two aliquots are required to determine the site-
177 specific isotopic composition of N₂O using the MAT-252, one for $\delta^{15}\text{N}^{\text{bulk}}$ and $\delta^{18}\text{O}$, and a

178 second for $\delta^{15}\text{N}^\alpha$ and $\delta^{15}\text{N}^\beta$. To determine $\delta^{15}\text{N}^{\text{bulk}}$ and $\delta^{18}\text{O}$ values, m/z 44, 45, and 46 (which
179 correspond to isotopologues of N_2O^+) are measured and compared with a standard. To determine
180 $\delta^{15}\text{N}^\alpha$ and $\delta^{15}\text{N}^\beta$ values, m/z 30 and 31 (which correspond to isotopologues of the electron
181 impact fragment ion NO^+) are measured. Determination of the ‘scrambling factor’ for an
182 instrument – i.e., the fraction of NO^+ in the sample being measured that included the β N-atom
183 (which is typically about 8% for the Finnegan 252 series [Yoshida and Toyoda, 1999; Kaiser et
184 al., 2004]) – allows the measurements of m/z 30, 31, 44, 45, and 46 to be combined to determine
185 values for $\delta^{15}\text{N}^\alpha$ and $\delta^{15}\text{N}^\beta$. Our 1σ measurement precisions are $\sim 0.2\text{‰}$ and 0.3‰ for
186 $\delta^{15}\text{N}^{\text{bulk}}$ and $\delta^{18}\text{O}$, respectively, and 0.8‰ and 0.9‰ for $\delta^{15}\text{N}^\alpha$ and $\delta^{15}\text{N}^\beta$, respectively.

187 **3. Results and Discussion**

188 Figure 1 shows the latitude and altitude distribution of the 125 samples from CRAVE and
189 TC^4 measured for N_2O isotope compositions. Measured values for $\delta^{15}\text{N}^{\text{bulk}}$, $\delta^{15}\text{N}^\alpha$, and $\delta^{18}\text{O}$ are
190 represented by the color scaling shown in the legends. The measurements are also given in Table
191 S1 in supplementary materials. As expected, the isotopic variability is small, with a range in δ -
192 values for each equivalent to ~ 4 times the corresponding 1σ measurement precision. While
193 below some of the interesting outliers (e.g., beyond 1 or 2σ) will be examined, it is instructive to
194 first examine the averaged vertical profiles for the different aircraft and missions. Figure 2 shows
195 the results for averaging the tropical data (i.e., $<11^\circ\text{N}$) in 1-km altitude bins, parsed and color-
196 coded by aircraft (WB-57 and DC-8) and campaign (CRAVE and TC^4). The error-bars shown
197 are the 1σ standard deviation of the average of the data for that altitude bin (solid bars) or, for the
198 few bins for which there is only a single datum, the measurement precision (dotted bars); the
199 number of samples per altitude bin is also indicated in Figure 2a in the corresponding color. For

200 comparison, the gray shading in each panel shows the $\pm 1\sigma$ (N=288 for $\delta^{15}\text{N}^{\text{bulk}}$ and $\delta^{18}\text{O}$ and
201 N=239 for $\delta^{15}\text{N}^{\alpha}$) variability in measured tropospheric N_2O isotopic compositions in air sampled
202 on the UC Berkeley campus (37.87°N, 122.26°W) between September 2001 and November
203 2006.

204 For $\delta^{15}\text{N}^{\text{bulk}}$, the average values and variability for the tropical profiles shown in Figure
205 2a fall within the range of those measured at the surface at midlatitudes at UC Berkeley. The
206 largest deviation appears in the lower stratosphere, where average $\delta^{15}\text{N}^{\text{bulk}}$ values increase; this is
207 shown more clearly in Figure 3 in which the measurements are binned into 0.5 km ranges and
208 then averaged. The increase in ^{15}N relative to ^{14}N in N_2O with altitude is due primarily to the
209 photolysis of N_2O in the stratosphere, which preferentially dissociates the $^{14}\text{N}^{14}\text{N}^{16}\text{O}$
210 isotopologue with a smaller contribution from photo-oxidation of N_2O by reaction with $\text{O}(^1\text{D})$
211 [e.g., *Blake et al.*, 2003; *Johnson et al.*, 2001; *Kaiser et al.*, 2002a; *Yung and Miller*, 1997]. As
212 the N_2O mixing ratios decrease with altitude in the stratosphere, the $\delta^{15}\text{N}^{\text{bulk}}$ values increase, as
213 expected. When the $\delta^{15}\text{N}^{\text{bulk}}$ and N_2O values for individual samples are plotted in a Rayleigh
214 isotope fractionation format in Figure 4 – i.e., as $\ln(1 + \delta^{15}\text{N}^{\text{bulk}}/1000)$ vs $\ln([\text{N}_2\text{O}]/[\text{N}_2\text{O}]_0)$ where
215 $[\text{N}_2\text{O}]_0$ is the N_2O mixing ratio for air entering the stratosphere – apparent fractionation
216 constants, ϵ_{app} , of $-15 \pm 7 \text{‰}$ and $-19 \pm 7 \text{‰}$ are obtained for CRAVE and TC⁴, respectively,
217 from the slope of the fit line. The uncertainties are large since the N_2O mixing ratios decrease by
218 only ~4 to 8 ppbv and the $\delta^{15}\text{N}^{\text{bulk}}$ values increase by only ~0.5‰ in the lowest 2 kilometers of
219 the stratosphere, which are intrinsically small and are close to the isotope measurement precision
220 of $\pm 0.2\text{‰}$. Nevertheless, these values for ϵ_{app} are within the range of -14 to -19‰ obtained in
221 the stratosphere for N_2O mixing ratios > 200 ppbv at 18°N [*Kaiser et al.*, 2006], midlatitudes
222 [e.g., *Toyoda et al.*, 2001; *Röckmann et al.*, 2001], and high latitudes [e.g., *Park et al.*, 2004]. As

223 discussed in the previous studies, these values for ϵ_{app} are at least a factor of two smaller than the
224 fractionation constant expected in an isolated system – that is, one in which chemistry alone is
225 acting to alter the isotopic composition and not transport or mixing of air of different isotopic
226 compositions. For example, a value of -34.7‰ is expected based on broadband photolysis of
227 N_2O at room temperature in the laboratory and a 10% contribution from N_2O oxidation by $\text{O}(^1\text{D})$
228 [Kaiser *et al.*, 2002a; Röckmann *et al.*, 2001]; transport and mixing decrease the slope of the
229 Rayleigh fractionation line, yielding a value for ϵ_{app} that is necessarily smaller than that for an
230 isolated system.

231 This isotope fractionation due to photolysis and photo-oxidation cannot be happening *in*
232 *situ* in the lowest 2 km of the tropical stratosphere, however. The lifetime of N_2O at altitudes
233 below 20 km in the tropics is ~ 70 years [Minschwaner *et al.*, 1993] and, thus, on the time scales
234 for tropical ascent, N_2O should not become enriched in ^{15}N . Rather, as shown previously using
235 measurements of the mixing ratios of a number of trace gas species below ~ 23 km,
236 photochemically-aged stratospheric air from midlatitudes must be transported and mixed
237 isentropically into the tropical upwelling region [e.g., Avallone and Prather, 1996; Boering *et*
238 *al.*, 1996; Volk *et al.*, 1996]; it is this mixing in of older air rather than *in situ* N_2O destruction
239 that results in the increasing ^{15}N enrichment in tropical N_2O with altitude above the tropopause
240 in Figure 3. For example, using the $\delta^{15}\text{N}^{\text{bulk}}$ measurements we can calculate a lower limit for the
241 vertical ascent rate in the lower tropical stratosphere during CRAVE assuming no in-mixing of
242 midlatitude air based on Rayleigh fractionation in an isolated system – i.e., by calculating how
243 long it would take to enrich N_2O from the average $\delta^{15}\text{N}^{\text{bulk}}$ value observed at 17.25 km to that
244 observed at 19.25 km based on the *in situ* destruction rate of N_2O . Using the fractionation
245 constant of -34.7‰ noted above and a 70-year lifetime for N_2O with respect to photolysis yields

246 an ascent rate of 0.063 mm s^{-1} (or 0.17 km/month), which would imply that air at 19.25 km took
247 at least 12 months to ascend to that altitude. In contrast, annually averaged vertical ascent rates in
248 the tropical lower stratosphere derived from observations of the propagation of annual cycles in
249 CO_2 [Boering *et al.*, 1996] and water vapor [e.g., Mote *et al.*, 1995] and from radiative
250 calculations [e.g., Eluszkiewicz *et al.*, 1995; Rosenlof *et al.*, 1996] are $\sim 0.2 \text{ mm s}^{-1}$ (~ 0.5
251 km/month) and are even larger ($\sim 0.35 \text{ mm s}^{-1} = 0.88 \text{ km/month}$) during northern winter when
252 the CRAVE samples were collected, indicating that the transit time for air from ~ 17 to 19 km is
253 on average 4 months, not 12 months, the value yielded by a Rayleigh model for an isolated lower
254 stratosphere. Using temperature-dependent rather than room temperature photolysis fractionation
255 constants, which gives an expected fractionation constant of -48 to -51% for the lower tropical
256 stratosphere [Kaiser *et al.*, 2002a; Kaiser *et al.*, 2002b], decreases that transit time to ~ 9 months,
257 a time scale that is still more than a factor of two larger than the generally accepted ascent time
258 scales noted above. Thus there is simply not enough time using a closed-system Rayleigh model
259 to enrich tropical N_2O in ^{15}N and requires that photochemically-processed air that is isotopically
260 enriched in ^{15}N has mixed into the tropics. In subsequent work, we will attempt to quantify this
261 in-mixing of midlatitude air as a function of altitude and compare it with previous estimates
262 based on tracer mixing ratio models. Finally, we note that an increase in $\delta^{18}\text{O}$ above the
263 tropopause (e.g., Figure 2c) is not as clear as for $\delta^{15}\text{N}^{\text{bulk}}$ and not apparent at all in $\delta^{15}\text{N}^{\alpha}$ (e.g.,
264 Figure 2b); this difference with respect to $\delta^{15}\text{N}^{\text{bulk}}$ is likely due to a fractionation constant for
265 $\delta^{18}\text{O}$ that is smaller than that for $\delta^{15}\text{N}^{\text{bulk}}$ by 10% and to a measurement precision that is 4 times
266 larger for $\delta^{15}\text{N}^{\alpha}$ than for $\delta^{15}\text{N}^{\text{bulk}}$ so that stratospheric enrichments may be masked by noise.

267 For $\delta^{18}\text{O}$, the averaged tropical profiles in Figure 2 show a remarkably consistent pattern
268 between the CRAVE and TC⁴ missions. At the lowest altitudes, N_2O is relatively depleted in ^{18}O ,

269 and is outside the $\pm 1\sigma$ range observed on average at the surface at UC Berkeley (gray shaded
270 area). Values for $\delta^{18}\text{O}$ then increase up to ~8 or 9 km and then generally decrease up to the
271 tropopause. Such repeatability between the two missions suggests that the profiles are
272 determined by an interplay of similar processes. One possibility is that the drivers underlying this
273 profile pattern are analogous to those for other species that exhibit a common “inverse C”-shaped
274 altitude profile that is determined by convection of surface air combined with chemistry and/or
275 mixing [e.g., *Prather and Jacob, 1997*]. For $\delta^{18}\text{O}$, an inverse C pattern could result from a source
276 of N_2O that is depleted in ^{18}O relative to the free troposphere at the surface, either from soils or
277 the ocean. Tropical convection takes this near-surface N_2O and deposits it at altitudes up to 10 to
278 14 km, thus leading to a decrease in $\delta^{18}\text{O}$ values at these higher altitudes influenced by
279 convective outflow. In between these altitudes, the air may be more characteristic of background
280 tropical and/or midlatitude air, with higher values of $\delta^{18}\text{O}$; the further from the surface source,
281 the more it resembles background air (i.e., $\delta^{18}\text{O}$ increases with altitude) until convective outflow
282 of surface air deposited higher altitudes begins to turn the profile back around towards lower
283 $\delta^{18}\text{O}$ values. The vertical profile for $\delta^{15}\text{N}^{\text{bulk}}$ (Figure 2a) does not show such a pattern, as
284 discussed above.

285 This difference in the $\delta^{18}\text{O}$ vs. $\delta^{15}\text{N}^{\text{bulk}}$ averaged profiles is consistent with two different
286 hypotheses for the isotopic composition of the source of N_2O that is influencing the trends in
287 isotopic compositions up to ~8 km. One hypothesis is that the major surface source of N_2O for
288 this region (e.g., oceanic or from soils) has an average $\delta^{18}\text{O}$ value that is significantly lower than
289 that for N_2O in background tropospheric air but has an average $\delta^{15}\text{N}^{\text{bulk}}$ value that is more similar
290 to that for N_2O in background tropospheric air. A second hypothesis is that two different surface
291 sources (e.g., one oceanic and one from soils) are both significant and are mixed together by

292 transport: both sources could have an average $\delta^{18}\text{O}$ value that is significantly lower than that for
293 N_2O in background tropospheric air, as in the first hypothesis, but one source could have $\delta^{15}\text{N}^\alpha$
294 values and low $\delta^{15}\text{N}^\beta$ values while the other source could have the reverse; the mixture of the two
295 sources would still result in lower values for $\delta^{18}\text{O}$ yet little variation in $\delta^{15}\text{N}^{\text{bulk}}$, since $\delta^{15}\text{N}^{\text{bulk}}$ is
296 an average of over the α and β sites. Furthermore, we note that the averaged profile for $\delta^{15}\text{N}^\alpha$
297 (Figure 2b) could be consistent with a surface source that is enriched in ^{15}N at the α position
298 since the data below 5 km appear to be isotopically heavier than the averaged data above these
299 altitudes, although such a pattern is arguably in the noise of the measurements.

300 Comparing these characteristics in the vertical profiles for $\delta^{18}\text{O}$, $\delta^{15}\text{N}^{\text{bulk}}$, and $\delta^{15}\text{N}^\alpha$ and
301 the two hypotheses outlined above with the range of isotopic compositions measured to date in
302 soils and the ocean suggests that the source that may be influencing the lower altitudes may be
303 more similar in isotopic composition to an ocean source than to a soil source, although a mixture
304 of the two cannot be ruled out. For example, the isotopic composition of N_2O in the subtropical
305 North Pacific gyre was measured by Popp *et al.* [2002] and indicates that N_2O transferred from
306 ocean to the air should be slightly depleted in bulk N and slightly more so in ^{18}O relative to the
307 background troposphere; they suggest a range for the ocean source of 3.5 to 5.5‰ for $\delta^{15}\text{N}^{\text{bulk}}$
308 and 35.5 to 41.5‰ for $\delta^{18}\text{O}$. Different ranges for the isotopic composition of emitted N_2O have
309 been measured in other ocean regions [e.g., Toyoda *et al.*, 2002]; in the absence of more
310 comprehensive ocean measurements and an understanding of what controls them, the ranges
311 relevant for this study will remain uncertain. In contrast, while there is great variability in
312 measurements of the isotopic composition of N_2O emitted from soils, in general it is significantly
313 more depleted in ^{15}N and ^{18}O relative to the tropospheric averages than an ocean source, and
314 significantly more so in $\delta^{15}\text{N}^{\text{bulk}}$ than in $\delta^{18}\text{O}$. For example, the emission weighted isotope

315 signature from unfertilized Costa Rican tropical rainforest soil $\delta^{15}\text{N}^{\text{bulk}} = -26 \pm 2.5\%$ and $\delta^{18}\text{O} =$
316 $26 \pm 6\%$ [Pérez *et al.*, 2000]. If a soil source of N_2O were the dominant factor determining the
317 lower $\delta^{18}\text{O}$ values in the lower altitudes of the vertical profile, then a signal in $\delta^{15}\text{N}^{\text{bulk}}$ would be
318 expected to be even stronger and yet such behavior appears to be absent, as noted above.
319 Furthermore, although measurements of the site-specific isotopic composition of oceanic N_2O
320 are even more rare than $\delta^{15}\text{N}^{\text{bulk}}$ and $\delta^{18}\text{O}$, Toyoda *et al.* [2002] have shown ocean profiles in
321 which $\delta^{15}\text{N}^{\alpha}$ values are large and $\delta^{15}\text{N}^{\beta}$ are small relative to background tropospheric air; as a
322 result, $\delta^{15}\text{N}^{\text{bulk}}$ values would be more similar to tropospheric air than either $\delta^{15}\text{N}^{\alpha}$ or $\delta^{15}\text{N}^{\beta}$.
323 Overall, these characteristics of ocean N_2O isotopic compositions seem more similar to the
324 trends and differences in the averaged profiles shown here than to a soil source, assuming the
325 averaged profiles are indeed representative of regional profiles in general.

326 Examining individual datapoints from the flight of 08 August 2007 may provide further
327 insight into the possible influence of a surface source on the isotopic composition of N_2O in the
328 tropical profiles. The DC-8 flight on this date included a dive over the Pacific Ocean into the
329 boundary layer, followed by an 11.5 km cruise and then a dive over the Colombian jungle.
330 Significant negative correlations exist between measurements of $\delta^{18}\text{O}$ of N_2O and the measured
331 mixing ratios of methyl iodide (CH_3I), methyl nitrate (CH_3ONO_2 or “ MeONO_2 ”), and ethyl
332 nitrate ($\text{C}_2\text{H}_5\text{ONO}_2$ or “ EtONO_2 ”), which are all tracers of marine convection, shown in Figure 5
333 a, b, and c. The descent over the Pacific showed the strongest negative correlations ($R = -0.714$,
334 -0.737 , and -0.725 for (a) MeONO_2 , (b) EtONO_2 , and (c) CH_3I , respectively, for a simple linear
335 least-squares regression). That these tracers of marine convection show a strong anti-correlation
336 in general with $\delta^{18}\text{O}$, and especially during the dive over the ocean, suggests that N_2O from the
337 ocean is influencing $\delta^{18}\text{O}$ of N_2O in the tropical profiles from both CRAVE and TC^4 .

338 Unfortunately, the range (or expected range based on IRMS peak areas) in N₂O mixing ratios are
339 too small [e.g., compare with CO₂ analyses in *Pataki et al.*, 2003] to allow a Keeling plot
340 analysis (in which the y-intercept of a plot of isotopic composition versus the reciprocal of the
341 mixing ratio yields an estimate of the isotopic composition of the “undiluted” source; Keeling
342 [1958]). Rather, only the tight correlation with the marine tracers is suggestive of an ocean link
343 for the source, or at least one of the sources, influencing the decrease in δ¹⁸O values towards the
344 surface in the profiles shown here. For δ¹⁵N^{bulk} and δ¹⁵N^α, however, the individual datapoints
345 show no significant correlation with the marine tracers (see Supplemental Figure S1).

346 For samples from the descent over the Colombian jungle, δ¹⁸O is strongly anti-correlated
347 with the surface tracers CO, CH₄, ethyne, benzene, and CH₃I, which is consistent with a soil or
348 an ocean source since both are depleted in ¹⁸O relative to background tropospheric N₂O; see
349 Supplementary Figure S1. (We note that only 1 whole air sample from an altitude of 1.5 km for
350 the jungle dive into the boundary layer was still available for isotopic analysis and it did not
351 display the highly elevated isoprene mixing ratios of many of the other boundary layer samples
352 taken at the bottom of the dive.) For δ¹⁵N^{bulk}, no correlation with surface tracers was observed,
353 analogous to the δ¹⁵N^{bulk}:ocean tracer correlations for the ocean dive (Figure S1). Interestingly,
354 however, there were strong positive correlations between δ¹⁵N^α and the surface tracers CO, CH₄,
355 ethyne, benzene, and CH₃I in the jungle dive. Such a positive correlation is not expected for a
356 soil source of N₂O. There are two interesting possibilities that might yield such positive
357 correlations based on details of the flight. One is that the N₂O isotopic composition still reflects
358 an ocean source (which is more likely to be enriched in δ¹⁵N^α); back trajectory calculations by
359 M. R. Schoeberl, P. A. Newman, and L. R. Lait (available through the NASA/ARC Earth
360 Science Project Office Archive at <http://espoarchive.nasa.gov>; see also Schoeberl and Sparling,

361 1995) suggest that the samples at 500 mbar pressure and lower altitudes had been over the
362 Atlantic within 2 to 7 days of the flight. Another possibility is based on observations by the DC-8
363 whole air sampler scientist that at the bottom of the Colombian jungle dive there were a
364 surprising number of swampy areas as well as cattle, both potential sources of N₂O enriched in
365 $\delta^{15}\text{N}^\alpha$ relative to a soil source and, most likely, the background troposphere as well. Thus, given
366 these two possible scenarios, it is unclear whether the positive correlations between $\delta^{15}\text{N}^\alpha$ and
367 the surface tracers are rather local (as might be expected from cows and swamps) or more
368 regional in nature (an ocean source, or mixture of ocean and soil). More measurements are
369 clearly needed to test these hypotheses. In general, however, we also note that it is rather
370 remarkable that there are large enough coherent variations in N₂O isotopic compositions with
371 respect to altitude and the mixing ratios of a number of surface tracers to even formulate the
372 hypotheses put forth here.

373 Another flight yielding interesting correlations between the measured N₂O isotopic
374 compositions and other atmospheric tracers was the WB-57 flight of 05 August 2007 from TC⁴.
375 Samples from this flight yielded several measurements of site-specific N₂O isotopologues that
376 showed a large deviation (4σ) from the average tropospheric values and a striking correlation
377 with greatly enhanced mixing ratios of several tracers indicative of industrial combustion or
378 biomass burning processes. The (unaveraged) altitude profiles for measurements of $\delta^{15}\text{N}^\alpha$ of
379 N₂O, ethane, propane, benzene, and tetrachloroethylene are shown in Figure 6a. The plume,
380 encountered at altitudes between 14 and 15 km is clearly visible. Trajectory-based convective
381 influence calculations provided by L. Pfister [*Pfister et al.*, 2001; Pfister, L., H. B. Selkirk, D.
382 O’C. Starr, P. A. Newman, and K. H. Rosenlof, A meteorological overview of the TC⁴ mission,
383 submitted to *J. Geophys. Res.*] suggest that these samples were likely affected by convection

384 within one day of the sampling, and that this convection was at least partially over Central
385 America, near Panama City, Panama. Figure 6b shows the anti-correlation between $\delta^{15}\text{N}^{\text{bulk}}$,
386 $\delta^{15}\text{N}^{\alpha}$, Site Preference (the relative enrichment at the α versus β nitrogen atom sites; see
387 Methods), and $\delta^{18}\text{O}$ of N_2O and the ethane mixing ratio for the 4 samples with the highest ethane
388 mixing ratios. Values for $\delta^{15}\text{N}^{\alpha}$ and Site Preference are very strongly anti-correlated with ethane
389 ($R = -0.9998$ and -0.9980 , respectively), consistent with both expectations for and
390 measurements of N_2O produced through biomass and fossil fuel combustion, which show that
391 N_2O produced by combustion processes is depleted in ^{15}N at the α nitrogen atom position
392 relative to the β nitrogen atom position [Toyoda *et al.*, 2008; Ogawa and Yoshida, 2005a,
393 2005b]. To our knowledge, this is the first time that N_2O isotope measurements in such a plume
394 influenced by combustion have been made in the remote atmosphere.

395 **4. Conclusions**

396 We have demonstrated that the isotopic composition of nitrous oxide varies throughout
397 the tropical troposphere with an average vertical structure in $\delta^{18}\text{O}$, discernible at current
398 measurement precision, but that is not observed in the ^{15}N measurements – characteristics that
399 are at least consistent with the influence of an oceanic source of N_2O on a regional scale, or
400 perhaps a mixture of ocean and soil sources. This hypothesis is supported by correlations
401 observed between $\delta^{18}\text{O}$ of N_2O and tracers of marine convection, which are particularly strong
402 during a dive over the ocean. In addition, we have further demonstrated the dramatic effect of an
403 industrial or biomass burning plume on the site-specific isotopic composition of N_2O . The
404 hypotheses put forth here regarding the sources of N_2O and the extent of their regional and
405 hemispheric influence on tropospheric profiles will require additional measurements to test them.
406 On the other hand, we note that it is somewhat surprising that the variability in observed N_2O

407 isotopic compositions and their coherent variations in altitude and with respect to a number of
408 surface tracers is large enough to at least formulate the hypotheses put forth here. Nevertheless,
409 the variations in the measurements of the isotopic composition of tropospheric N₂O reported here
410 are small compared to the measurement precision - the range of measured isotopic composition
411 is only around 4 σ - suggesting that improvements in analytical techniques (and/or using the more
412 time-consuming dual inlet IRMS technique of Kaiser et al. [2003]) would be useful, allowing
413 more information to be extracted from the data. Ultimately, these measurements are “proof-of-
414 concept” that persistent and coherent variations in atmospheric N₂O isotopic compositions are
415 measurable and could aid in using, e.g., inverse models to constrain the sources of N₂O on
416 hemispheric to regional scales. Such modeling capabilities will be highly desirable not only for
417 greenhouse gas concentration predictions and feedbacks but also for verification of future
418 adherence to, e.g., Kyoto Protocol-like international agreements for N₂O emissions.

419

420 **Acknowledgments:** We gratefully acknowledge support from the NASA Upper Atmosphere
421 Research Program (NNG05G010G to UC Berkeley) and to U Miami, the NASA Tropospheric
422 Chemistry Program, and a Dreyfus Teacher-Scholar Award for KAB. We also thank R. Lueb for
423 support in sample collection, Aaron Johnson for isotope measurements assistance, X. Zhu and L.
424 Pope for laboratory work, G. Sachse and C. Harward for DACOM data, and L. Pfister of NASA
425 Ames Research Center and M. Schoeberl, P. Newman, and L. Lait of the Atmospheric Chemistry
426 and Dynamics Branch of the NASA Goddard Space Flight Center for convective influence and
427 back trajectory calculations.

428 **References**

- 429 Andrews, A. E., K. A. Boering, B. C. Daube, S. C. Wofsy, E. J. Hints, E. M. Weinstock, and T.
430 P. Bui (1999), Empirical age spectra for the lower tropical stratosphere from in situ
431 observations of CO₂: Implications for transport, *J. Geophys. Res.*, *104* (D21), 26581-
432 26595.
- 433 Avalone, L. M. and M. J. Prather (1996), Photochemical evolution of ozone in the lower tropical
434 stratosphere, *J. Geophys. Res.*, *101*(D1), 1457-1461.
- 435 Bernard, S., T. Roeckmann, J. Kaiser, J.-M. Barnola, H. Fischer, T. Blunier, and J. Chappellaz
436 (2006), Constraints on N₂O budget changes since pre-industrial time from new firn air
437 and ice core isotope measurements, *Atmos. Chem. Phys.*, *6*, 493-503.
- 438 Blake, G. A., M.-C. Liang, C. G. Morgan, and Y. L. Yung (2003), A Born-Oppenheimer
439 photolysis model of N₂O fractionation, *Geophys. Res. Lett.*, *30*(12), 1656,
440 doi:10.1029/2003GL016932.
- 441 Blake, N. J., D. R. Blake, A. L. Swanson, E. L. Atlas, F. Flocke, and F. S. Rowland (2003),
442 Latitudinal, vertical, and seasonal variations of C₁-C₄ alkyl nitrates in the troposphere
443 over the Pacific Ocean during PEM-Tropics A and B: Oceanic and continental sources, *J.*
444 *Geophys. Res.*, *108* (D2), 8242-8255.
- 445 Blake, N. J., et al. (1999), Aircraft measurements of the latitudinal, vertical, and seasonal
446 variations of NMHCs, methyl nitrate, methyl halides, and DMS during the First Aerosol
447 Characterization Experiment (ACE 1), *J. Geophys. Res.*, *104* (D17), 21803-21818.
- 448 Boering, K. A., S. C. Wofsy, B. C. Daube, H. R. Schneider, M. Lowenstein, J. R. Podolske and
449 T. J. Conway (1996), Stratospheric mean ages and transport rates from observations of
450 carbon dioxide and nitrous oxide, *Science*, *274*, 1340-1343.

451 Bol, R., S. Toyoda, S. Yamulki, J. M. B. Hawkins, L. M. Cardenas, and N. Yoshida (2003), Dual
452 isotope and isotopomer ratios of N₂O emitted from a temperate grassland soil after
453 fertilizer application, *Rapid Commun. Mass Spectrom.*, *17*, 2550-2556.

454 Cantrell, C. A. (2008), Technical Note: Review of methods for linear least-squares fitting of data
455 and application to atmospheric chemistry problems, *Atmos. Chem. Phys.*, *8*, 5477-5487.

456 Colman, J. J., A. L. Swanson, S. Meinardi, and D. R. Blake (2001), Description of the analysis of
457 a wide range of volatile organic compounds in whole air samples collected during PEM-
458 Tropics A and B, *Anal. Chem.*, *73*, 3273-3731.

459 Flocke, F., et al. (1999), An examination of chemistry and transport processes in the tropical
460 lower stratosphere using observations of long-lived and short-lived compounds obtained
461 during STRAT and POLARIS, *J. Geophys. Res.*, *104*(D21), 26,625–26,642.

462 Forster, P., et al.(2001), In *Climate Change 2007: The Physical Science Basis*; Solomon, S., Qin,
463 D., Manning, M., Chen, Z., Marquis, M., Averyt, K. B., Tignor, M., and Miller, H. L.,
464 Eds.; Cambridge University Press: Cambridge U.K.

465 Griffith, D. W. T., S. D. Parkes, V. Haverd, C. Paton-Walsh, and S. R. Wilson (2009), Absolute
466 calibration of the intramolecular site preference of ¹⁵N fractionation in tropospheric N₂O
467 by FT-IR spectroscopy, *Anal. Chem.*, *81*(6), 2227–2234.

468 Hirsch, A. I., A. M. Michalak, L. M. Bruhwiler, W. Peters, E. J. Dlugokencky, and P. P. Tans
469 (2006), Inverse modeling estimates of the global nitrous oxide surface flux from 1998–
470 2001, *Global Biogeochem. Cycles*, *20*, GB1008.

471 Hurst, D. F., et al. (2002), Construction of a unified, high-resolution nitrous oxide data set for
472 ER-2 flights during SOLVE, *J. Geophys. Res.*, *105*(D15), 19,811-19,822.

473 Jiang, X, W. L. Ku, R.-L. Shia, Q. Li, J. W. Elkins, R. G. Prinn, Y. L. Yung (2007), Seasonal
474 cycle of N₂O: Analysis of data, *Global Biogeochem. Cycles*, 21, GB1006.

475 Johnson, M. S., G. D. Billing, A. Groudis, M. H. M. Janssen (2001), Photolysis of nitrous oxide
476 isotopomers studied by time-dependent Hermite propagation, *J. Phys. Chem. A*, 105,
477 8672-8680, doi:10.1021/jp011449x.

478 Kaiser, J., C. A. M. Brenninkmeijer, and T. Röckmann (2002a) Intramolecular ¹⁵N and ¹⁸O
479 fractionation in the reaction of N₂O with O(¹D) and its implications for the stratospheric
480 N₂O isotope signature, *J. Geophys. Res.*, 107(D14), 4214, doi:10.1029/2001JD001506.

481 Kaiser, J., T. Röckmann, and C. A. M. Brenninkmeijer (2002b), Temperature dependence of
482 isotope fractionation in N₂O photolysis, *Phys. Chem. Chem. Phys.*, 4, 4420-4430.

483 Kaiser, J., S. Park, K. A. Boering, C. A. M. Brenninkmeijer, A. Hilkert, and T. Röckmann
484 (2004), Mass spectrometric method for the absolute calibration of the intramolecular
485 nitrogen isotope distribution in nitrous oxide, *Anal. Bioanal. Chem.*, 378, 256-269.

486 Kaiser, J., T. Röckmann, and C. A. M. Brenninkmeijer (2003), Complete and accurate mass
487 spectrometric isotope analysis of tropospheric nitrous oxide, *J. Geophys. Res.*, 108 (D15),
488 4476-4492.

489 Kaiser, J., A. Engel, R. Borchers, and T. Röckmann (2006), Probing stratospheric transport and
490 chemistry with new balloon and aircraft observations of the meridional and vertical N₂O
491 distribution, *Atmos. Chem. Phys.*, 6, 3535-3556.

492 Keeling, C. D. (1958), The concentration and isotopic abundances of atmospheric carbon dioxide
493 in rural areas, *Geochim. Cosmochim. Acta*, 13, 322-334.

494 Kim, K.-R. and H. Craig (1993), Nitrogen-15 and oxygen-18 characteristics of nitrous oxide: A
495 global perspective, *Science*, 262, 1855-1857.

496 MacFarling Meure, C., D. M. Etheridge, C. M. Trudinger, L. P. Steele, R. L. Langenfelds, T. van
497 Ommen, A. Smith, and J. W. Elkins (2006), Law Dome CO₂, CH₄, and N₂O ice core
498 records extended to 2000 years BP, *Geophys. Res. Lett.*, *33*, L14810.

499 Minschwaner, K., R. J. Salawitch, and M. B. McElroy (1993), Absorption of solar radiation by
500 O₂: Implications for O₃ and lifetimes of N₂O, CFCl₃ and CF₂Cl₂, *J. Geophys. Res.*,
501 *98*(D6), 10,543-10,561.

502 Nevison, C. D., R. F. Keeling, R. F. Weiss, B. N. Popp, X. Jin, P. J. Fraser, L. W. Porter, and P.
503 G. Hess (2005), Southern ocean ventilation inferred from seasonal cycles of atmospheric
504 N₂O and O₂/N₂ at Cape Grim, Tasmania, *Tellus*, *57B*, 218-229.

505 Nevison, C. D., N. M. Mahowald, R. F. Weiss, R. G. Prinn (2007), Interannual and seasonal
506 variability in atmospheric N₂O, *Global Biogeochem. Cycles*, *21*, GB3017,.

507 Ogawa, M., and N. Yoshida (2005a), Intramolecular distribution of stable nitrogen and oxygen
508 isotopes of nitrous oxide emitted during coal combustion, *Chemosphere*, *61*, 877-887.

509 Ogawa, M., and N. Yoshida (2005b), Nitrous oxide emission from the burning of agricultural
510 residue, *Atmos. Environ.*, *39*, 3421-3429.

511 Park, S., E. L. Atlas, and K. A. Boering (2004), Measurements of N₂O isotopologues in the
512 stratosphere: Influence of transport on the apparent enrichment factors and the
513 isotopologue fluxes to the troposphere, *J. Geophys. Res.*, *109*, D01305.

514 Park, S., K. A. Boering, D. M. Etheridge, D. Forretti, K.-R. Kim, R. L. Langenfelds, T. van
515 Ommen, L. P. Steele, and C. M. Trudinger (2005), Trends in the Nitrogen and Oxygen
516 Isotopic Compositions of Tropospheric Nitrous Oxide and Implications for the Global
517 Budget, *Eos Trans.*, *86* (52), Abstract A44B-03.

518 Park, S., et al. (2008), Trends, seasonal cycles, and interannual variability in the isotopic
519 composition of nitrous oxide between 1940 and 2008, *Eos Trans.*, 89 (53), Abstract
520 A21A-0125.

521 Pataki, D. E., J. R. Ehleringer, L. B. Flanagan, D. Yakir, D. R. Bowling, C. J. Still, N.
522 Buchmann, J. O. Kaplan, and J. A. Berry (2003), The application and interpretation of
523 Keeling plots in terrestrial carbon cycle research, *Global Biogeochem. Cycles*, 17(1),
524 1022.

525 Pérez, T., S. E. Trumbore, S. C. Tyler, E. A. Davidson, M. Keller, and P. B. de Camargo (2000),
526 Isotopic Variability of N₂O Emissions From Tropical Forest Soils, *Global Biogeochem.*
527 *Cycles*, 14(2), 525–535.

528 Pérez, T., S. E. Trumbore, S. C. Tyler, P. A. Matson, I. Ortiz-Monasterio, T. Rahn, and D. W. T.
529 Griffith (2001), Identifying the agricultural imprint on the global N₂O budget using stable
530 isotopes, *J. Geophys. Res.*, 106(D9), 9869–9878.

531 Pérez, T., D. Garcia-Montiel, S. Trumbore, S. Tyler, P. de Camargo, M. Moriera, M. Piccolo,
532 and C. Cerri (2006), Nitrous oxide nitrification and denitrification ¹⁵N enrichment factors
533 from Amazon forest soils, *Ecol. Appl.*, 16(6), 2153-2167.

534 Pfister, L., et al. (2001), Aircraft observations of thin cirrus clouds near the tropical tropopause,
535 *J. Geophys. Res.*, 106(D9), 9765-9786.

536 Popp, B. N., et al. (2002), Nitrogen and oxygen isotopomeric constraints on the origins and sea-
537 to-air flux of N₂O in the oligotrophic subtropical North Pacific gyre, *Global Biogeochem.*
538 *Cycles*, 16 (4), 1064-1073.

539 Prather, M. J., and D. J. Jacob (1997), A persistent imbalance in HO_x and NO_x photochemistry of
540 the upper troposphere driven by deep tropical convection, *Geophys. Res. Lett.*, 24(24),
541 3189-3192.

542 Rahn, T., and M. Wahlen (2000), A reassessment of the global budget of atmospheric nitrous
543 oxide, *Global Biogeochem. Cycles*, 14(2), 537-543.

544 Röckmann, T., and I. Levin (2005), High-precision determination of the changing isotopic
545 composition of atmospheric N₂O from 1990 to 2002, *J. Geophys. Res.*, 110, D21304.

546 Röckmann, T., J. Kaiser, C. A. M. Brenninkmeijer, J. N. Crowley, R. Borchers, W. A. Brand,
547 and P. J. Crutzen (2001), Isotopic enrichment of nitrous oxide (¹⁵N¹⁴NO, ¹⁴N¹⁵NO,
548 ¹⁴N¹⁴N¹⁸O) in the stratosphere and in the laboratory, *J. Geophys. Res.*, 106(D10), 10,403-
549 10,410.

550 Sachse, G. W., G. F. Hill, L. O. Wade, and M. G. Perry (1987), Fast-response, high precision
551 carbon monoxide sensor using a tunable diode laser absorption technique, *J. Geophys.*
552 *Res.*, 92, 2071-2081.

553 Sachse, G. W., J. E. Collins, G. F. Hill, L. O. Wade, L. G. Burney, and J. A. Ritter (1991),
554 Airborne tunable diode laser sensor for high precision concentration and flux
555 measurements of carbon monoxide and methane, *Proc. SPIE Int. Opt. Eng.*, 1433, 145-
556 156.

557 Schoeberl, M. R. and Sparling, L. (1995), Trajectory Modeling, in: Diagnostic Tools in
558 Atmospheric Physics, edited by: Fiocco, G. and Visconti, G., Proceedings of the
559 International School of Physics "Enrico Fermi", 124, 289-306.

560

561 Sowers, T., A. Rodebaugh, N. Yoshida, and S. Toyoda (2002), Extending the records of the
562 isotopic composition of atmospheric N₂O back to 1800 A.D. from firn air trapped in
563 snow at the South Pole and the Greenland Ice Sheet Project II ice core, *Global*
564 *Biogeochem. Cycles*, 16 (4), 1129-1138.

565 Toyoda, S., S.-I. Yamamoto, S. Arai, H. Nara, N. Yoshida, K. Kashiwakura, and K.-I. Akiyama
566 (2008), Isotopomeric characterization of N₂O produced, consumed, and emitted by
567 automobiles, *Rapid Commun. Mass Spectrom.*, 22, 603-312.

568 Toyoda, S., and N. Yoshida (1999), Determination of nitrogen isotopomers of nitrous oxide on a
569 modified isotope ratio mass spectrometer, *Anal. Chem.*, 71, 4711-4718.

570 Toyoda, S., N. Yoshida, T. Urabe, S. Aoki, T. Nakazawa, S. Sugawara, and H. Honda (2001),
571 Fractionation of N₂O isotopomers in the stratosphere, *J. Geophys. Res.*, 106(D7), 7515-
572 7522.

573 Toyoda, S., N. Yoshida, T. Miwa, Y. Matsui, H. Yamagishi, U. Tsunogai, Y. Niojiri, and N.
574 Tsurushima (2002), Production mechanism and global budget of N₂O inferred from its
575 isotopomers in the western North Pacific, *Geophys. Res. Lett.*, 29(3), doi:
576 10.1029/2001GL014311.

577 Volk, C. M., et al. (1996), Quantifying transport between the tropical and mid-latitude lower
578 stratosphere, *Science*, 272, 1763-1768.

579 Westley, M. B., B. N. Popp, and T. M. Rust (2007), The calibration of the intramolecular
580 nitrogen isotope distribution in nitrous oxide measured by isotope ratio mass
581 spectrometry, *Rapid Commun. Mass Spectrom.*, 21, 391-405.

582 Yung, Y.L., and C.E. Miller (1997), Isotopic fractionation of stratospheric nitrous oxide,
583 *Science*, 278, 1778-1780.

584 **Figure captions**

585 **Figure 1:** Whole air samples analyzed for the isotopic composition of N₂O for the CRAVE and
586 TC⁴ missions. Symbols show sampling location given by altitude (y-axis) vs latitude (x-
587 axis) for the CRAVE WB-57 samples (squares), TC⁴ WB-57 samples (triangles), and TC⁴
588 DC-8 samples (circles), colorscaled by the isotopic composition of N₂O: (a) $\delta^{15}\text{N}^{\text{bulk}}$, (b)
589 $\delta^{15}\text{N}^{\alpha}$ and (c) $\delta^{18}\text{O}$.

590 **Figure 2:** Vertical profiles of the isotopic composition of N₂O for samples collected at latitudes
591 <11°N: (a) $\delta^{15}\text{N}^{\text{bulk}}$, (b) $\delta^{15}\text{N}^{\alpha}$, and (c) $\delta^{18}\text{O}$ for the CRAVE WB-57 samples (circles), the
592 TC⁴ WB-57 samples (triangles), and the TC⁴ DC-8 samples (squares). Measured values
593 were binned and averaged in 1-km intervals. Error bars in each panel show the standard
594 deviation of the mean for each bin, while the numbers in (a) give the number of samples
595 in each bin; bins for which there is only one sample are indicated by dashed error bars.

596 **Figure 3:** Vertical profiles of the mixing ratio (open symbols) and $\delta^{15}\text{N}^{\text{bulk}}$ (closed symbols) of
597 N₂O, averaged into 0.5 km bins for samples collected at latitudes <11°N and altitudes
598 >15km for (a) CRAVE and (b) TC⁴.

599 **Figure 4:** Individual measurements of $\delta^{15}\text{N}^{\text{bulk}}$ of N₂O for samples from the tropical lower
600 stratosphere (<11°N and > 17 km) for (a) CRAVE and (b) TC⁴ are shown here plotted in
601 a Rayleigh isotope fractionation format, i.e., as $\ln(1 + \delta^{15}\text{N}^{\text{bulk}}/1000)$ vs $\ln([\text{N}_2\text{O}]/[\text{N}_2\text{O}]_0)$,
602 where $[\text{N}_2\text{O}]_0$ is the N₂O mixing ratio for air entering the stratosphere.

603 **Figure 5:** Tracer-tracer plots of $\delta^{18}\text{O}$ of N₂O vs mixing ratios of (a) MeONO₂, (b) EtONO₂, and
604 (c) CH₃I from the 08 August 2007 DC-8 samples, parsed into sections of the flight
605 corresponding to a dive over the Pacific (circles; latitude = 4.3 to 5.2°N, longitude = 79.1
606 to 83.1°W, altitude = 0.5 to 11.6 km), a dive over the Colombian jungle (triangles;

607 latitude = 1.6 to 3.0°N, longitude = 70.5 to 79.1°W, altitude = 1.5 to 11.6 km), and the
608 DC-8 cruise region in between (squares; latitude = 3.4 to 4.3°N, longitude = 71.9 to
609 79.1°W, altitude = 11.6 km). The value of the correlation coefficient, r , is given in the
610 figure legends, while the regression line is shown for the Pacific dive data.

611 **Figure 6:** (a) Vertical profiles of the mixing ratios of propane (black; in pptv), ethane (red; in
612 pptv and offset by 500 pptv), benzene (blue; in 100×pptv and offset by 2000 pptv), and
613 tetrachloroethylene (C₂Cl₄, green; in pptv, upper x-axis) from the WB-57 flight of 05
614 August 2007; solid symbols show the samples designated here as being in the combustion
615 plume at ~14 km altitude. (b) Correlation between the N₂O isotopic composition and the
616 ethane mixing ratio ($\delta^{15}\text{N}^{\text{bulk}}$: red squares; $\delta^{15}\text{N}^{\alpha}$: green triangles; Site Preference (see
617 text): blue circles; and $\delta^{18}\text{O}$: black diamonds for the combustion plume samples in (a).

618
619

FIGURE 1 (a and b):

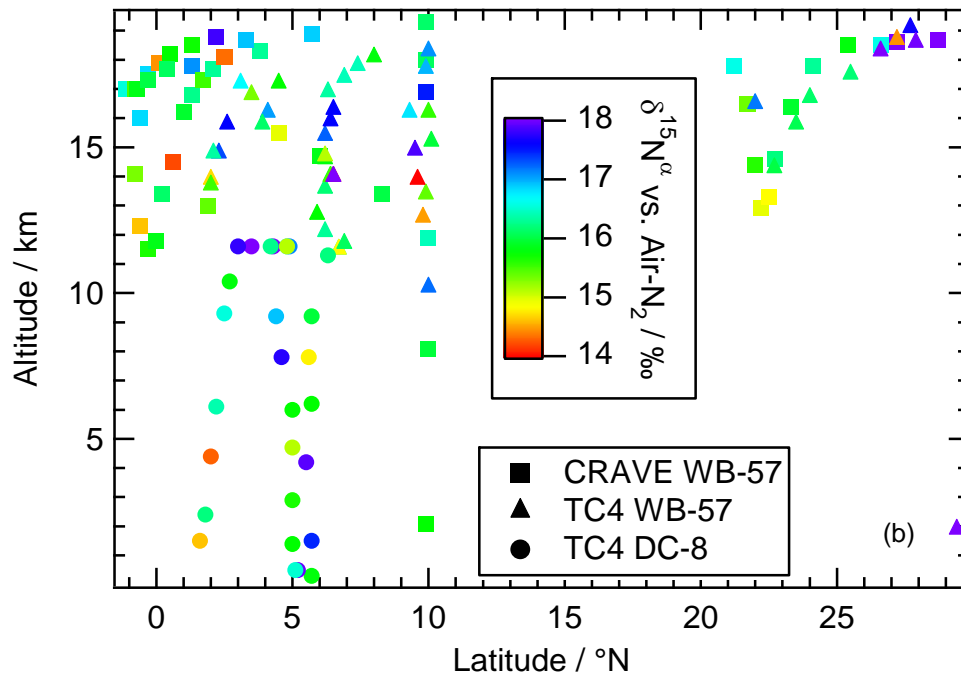
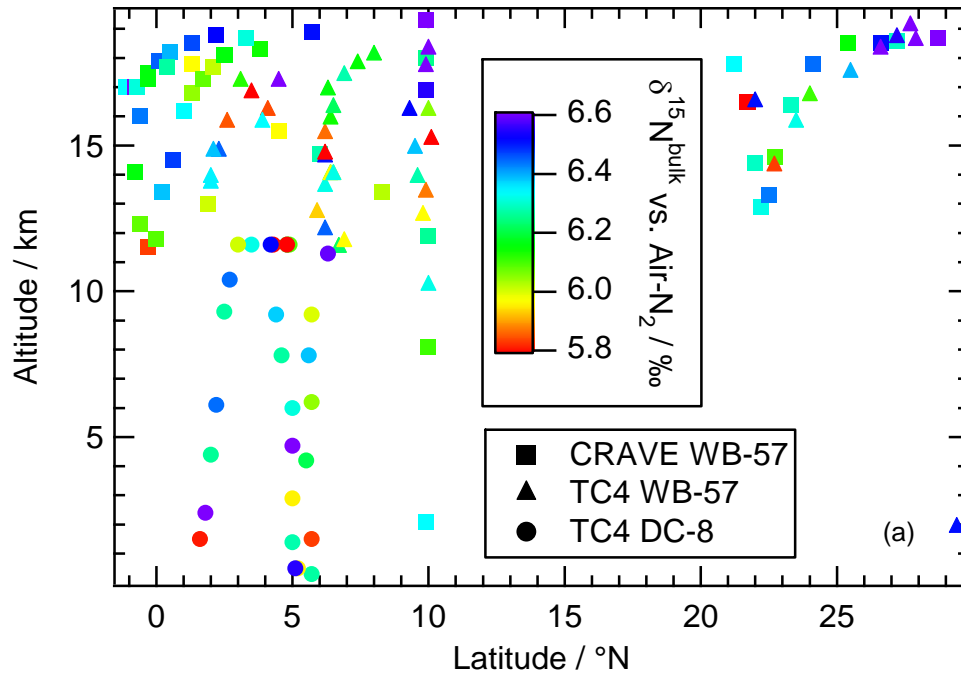


FIGURE 1 (c)

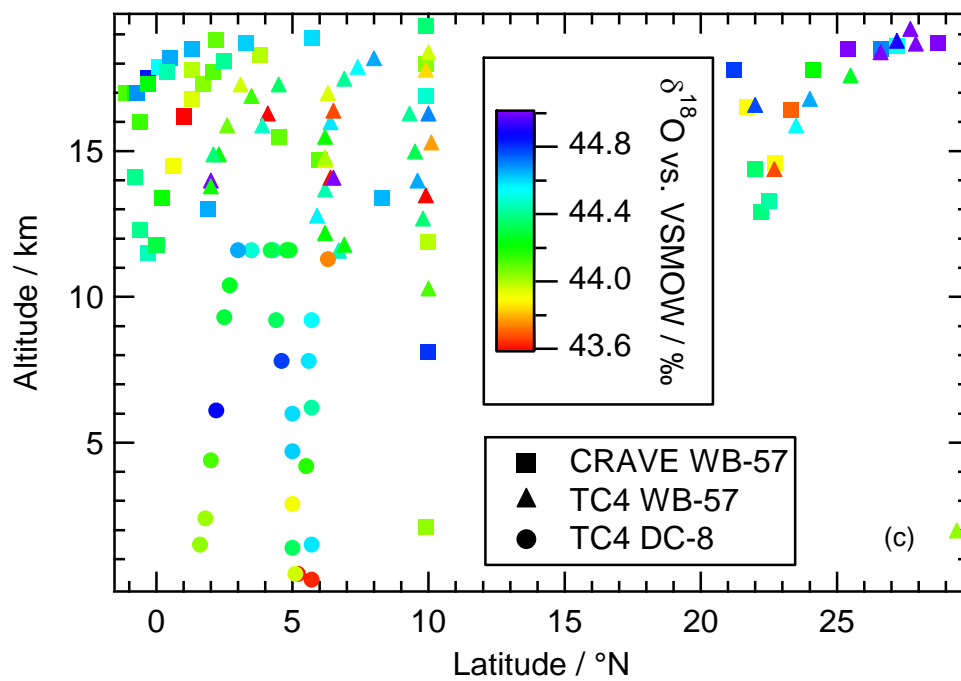


FIGURE 2:

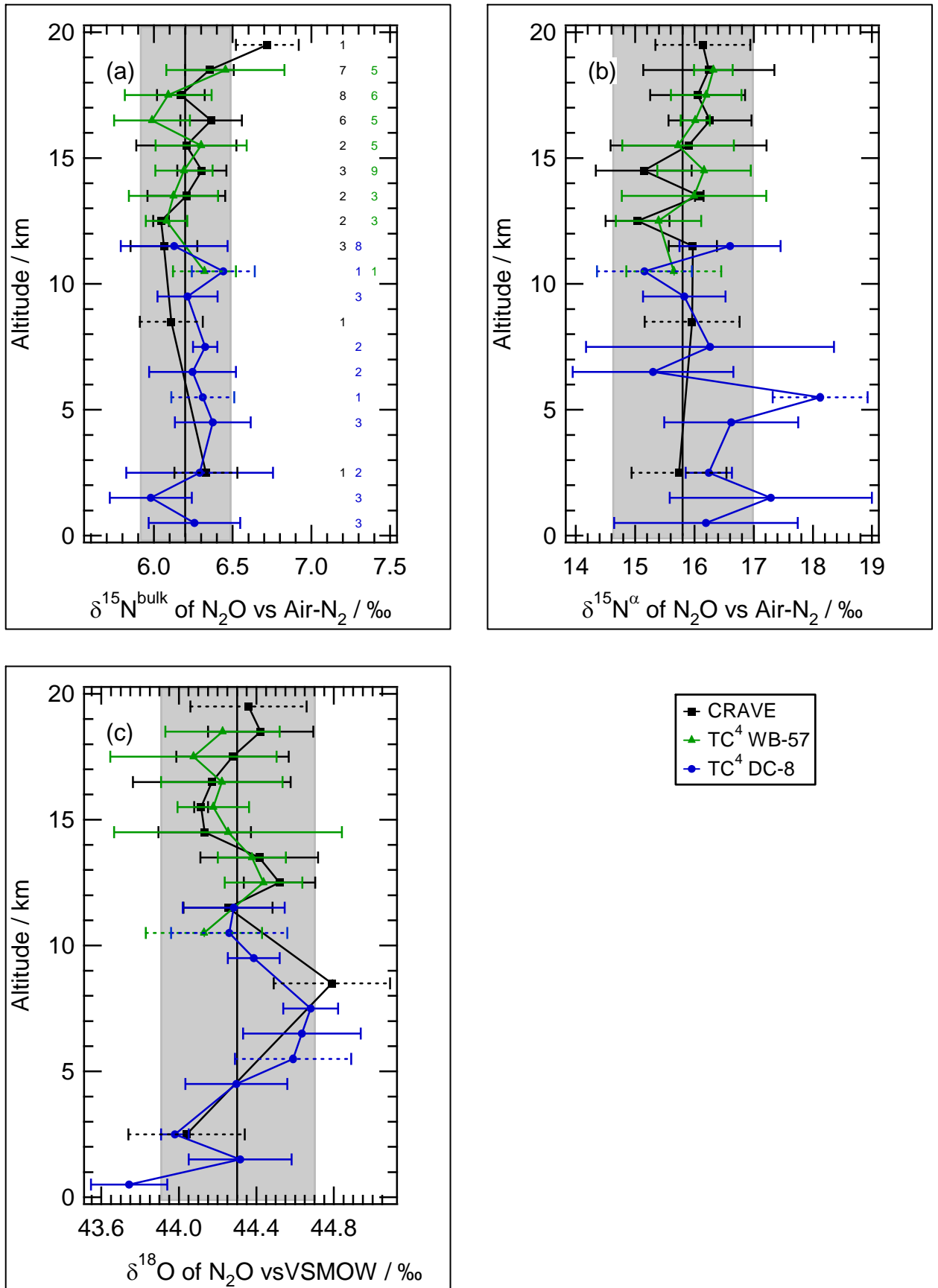


FIGURE 3:

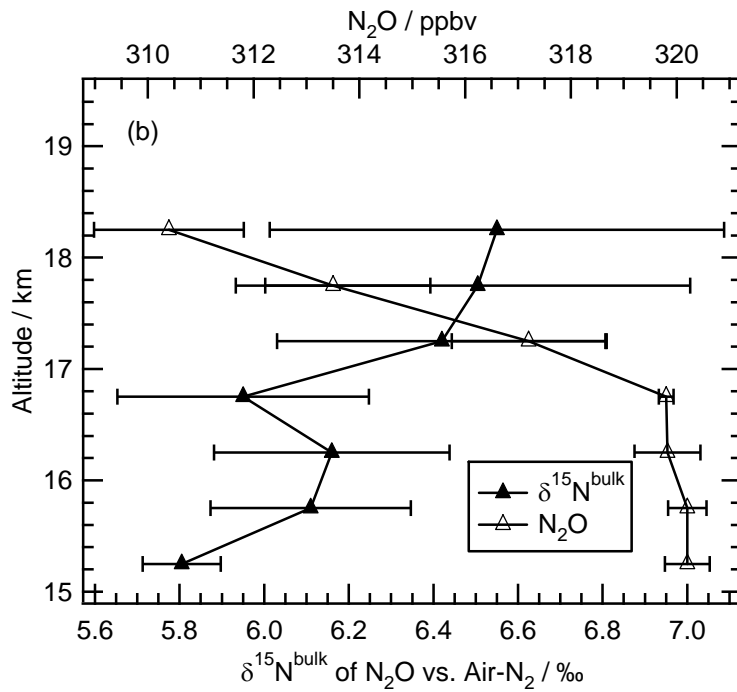
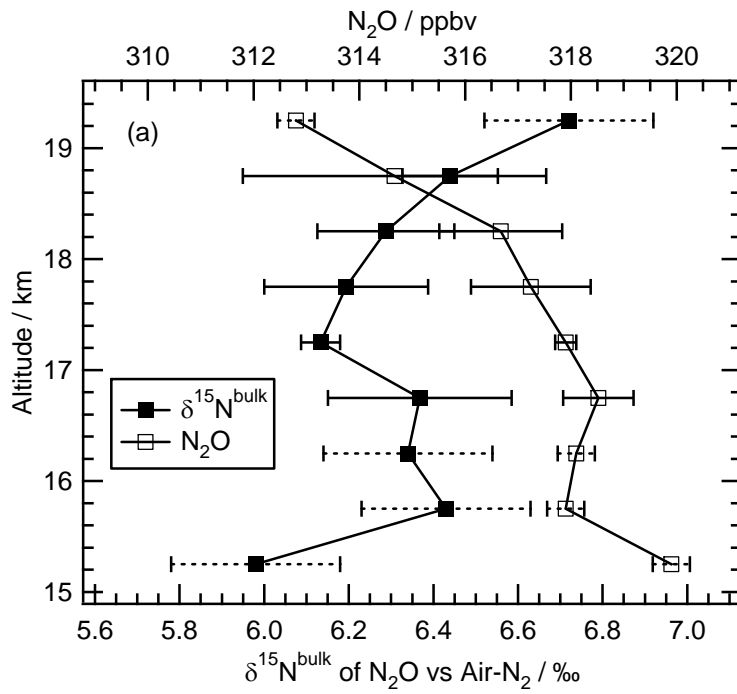


FIGURE 4:

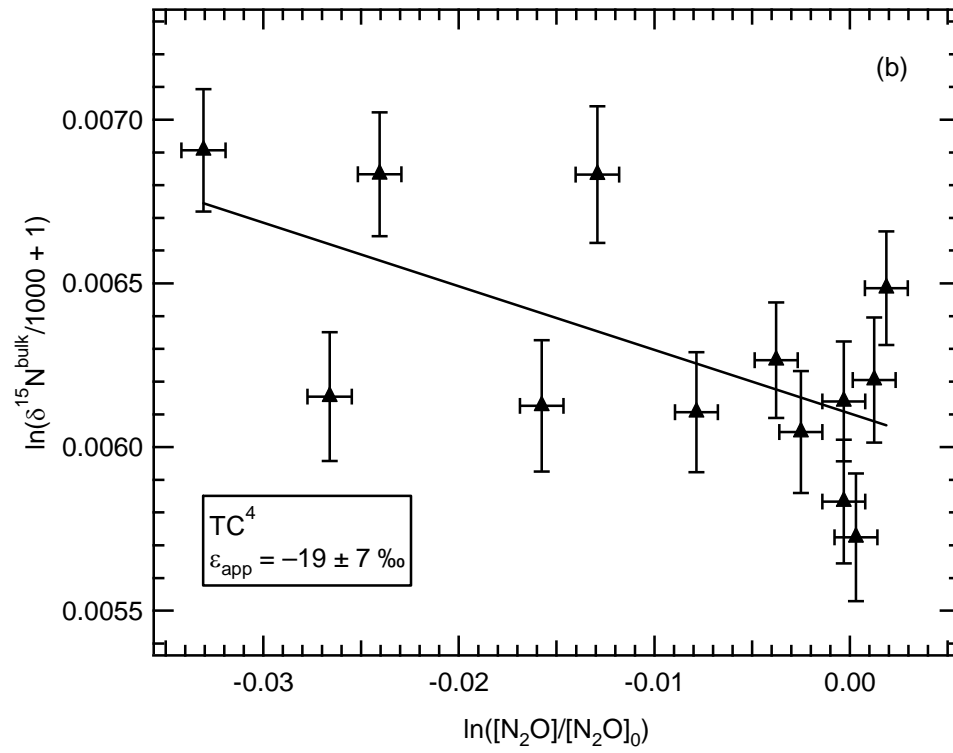
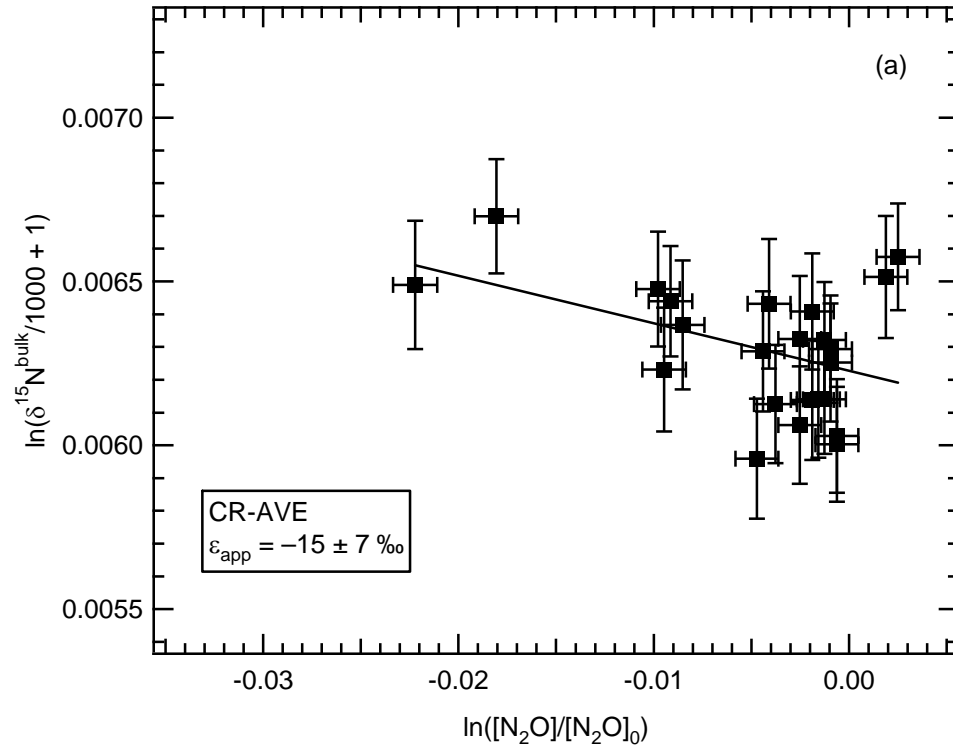


FIGURE 5:

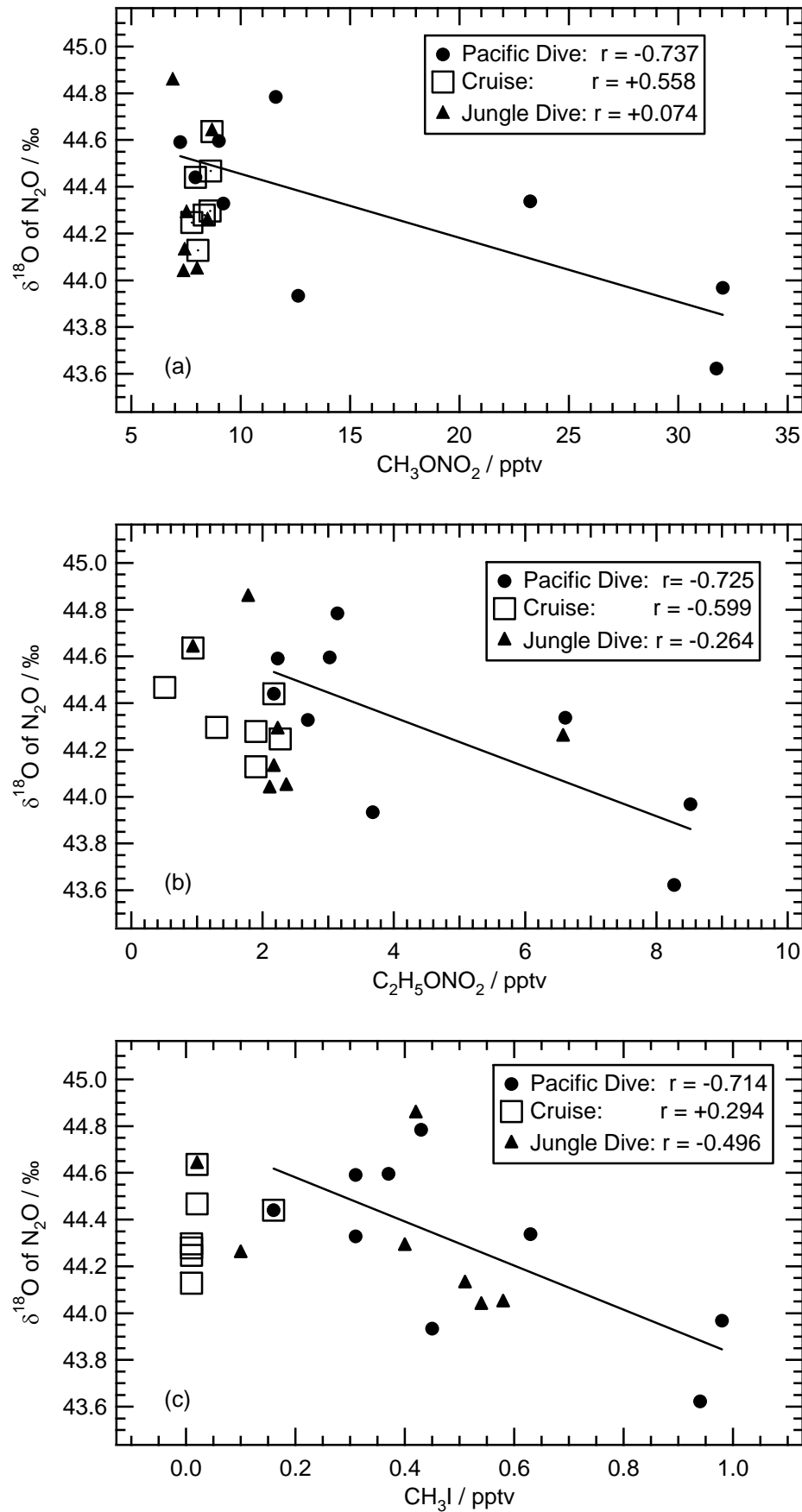
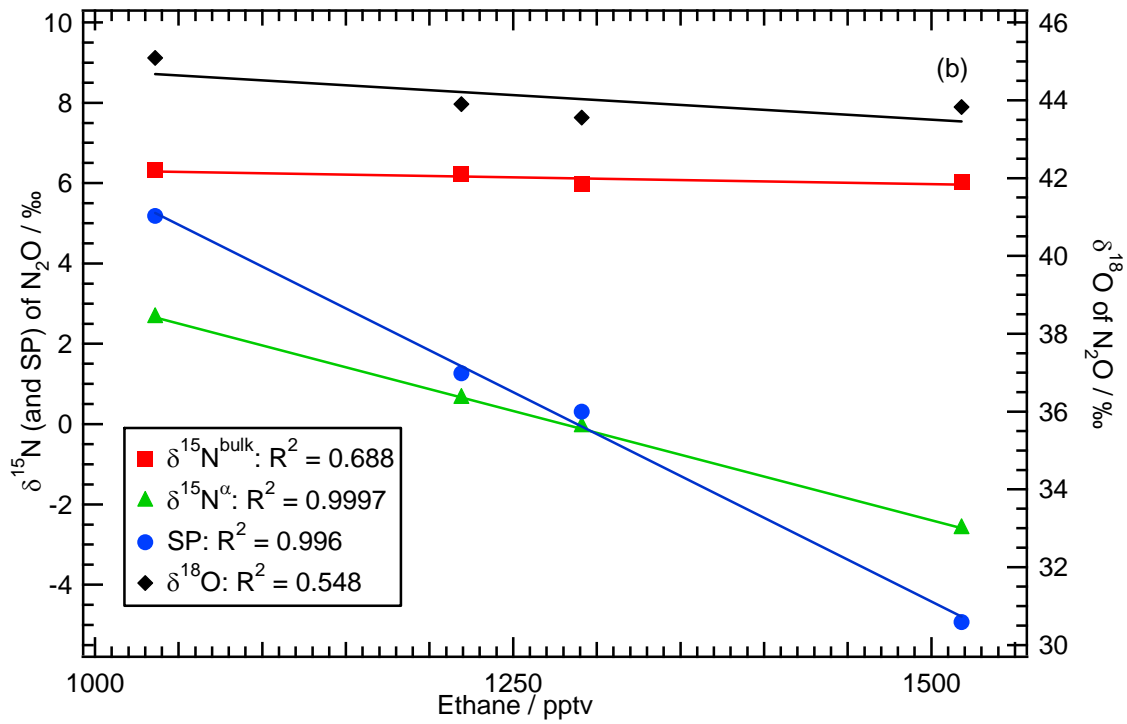
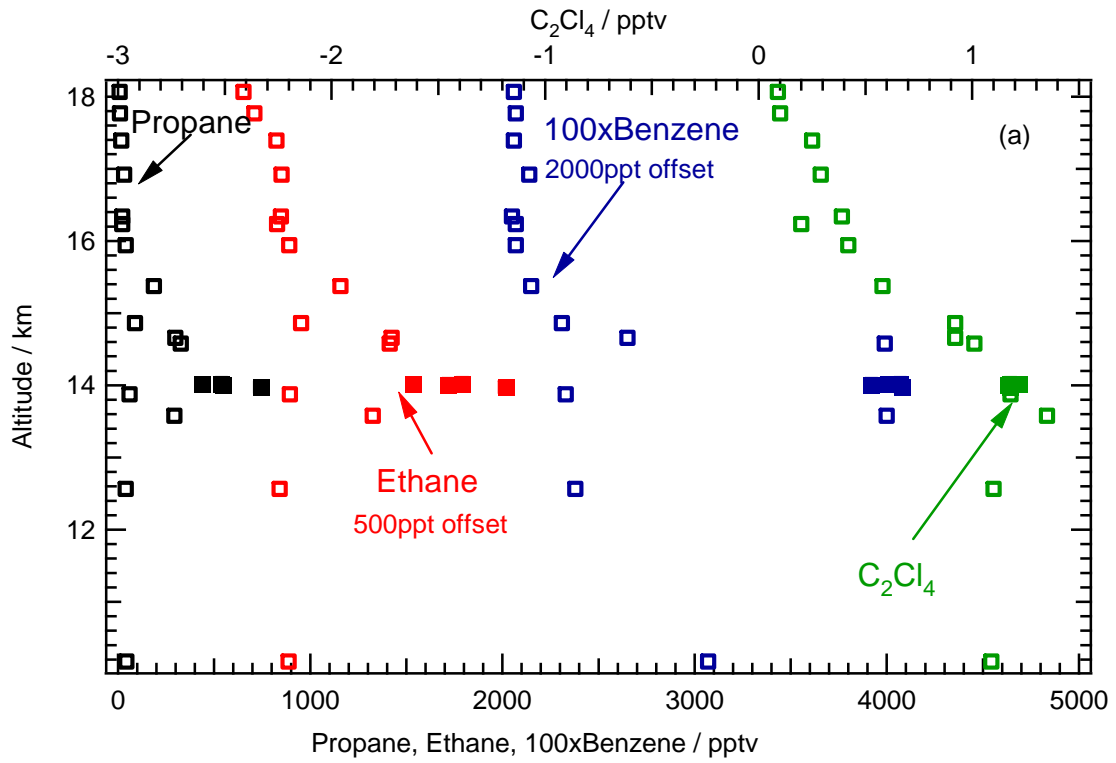


FIGURE 6:



SUPPLEMENTARY MATERIALS (3 figures, 4 tables)

Supplementary Figure Captions:

Figure S1: Correlations between $\delta^{15}\text{N}^{\text{bulk}}$ of N_2O versus various tracers for the DC-8 flight segments on 08 August 2007 over the Pacific Ocean (black squares) and the Colombian jungle (red triangles), color-coded by altitude. Values for the correlation coefficient, r , are given in the figure. See Figure 5 caption for additional information; the data are given in Supplementary Tables S3 and S4.

Figure S2: The same as for Figure S1 but for $\delta^{15}\text{N}^{\alpha}$ of N_2O .

Figure S3: The same as for Figure S1 but for $\delta^{18}\text{O}$ of N_2O .

Figure S1:

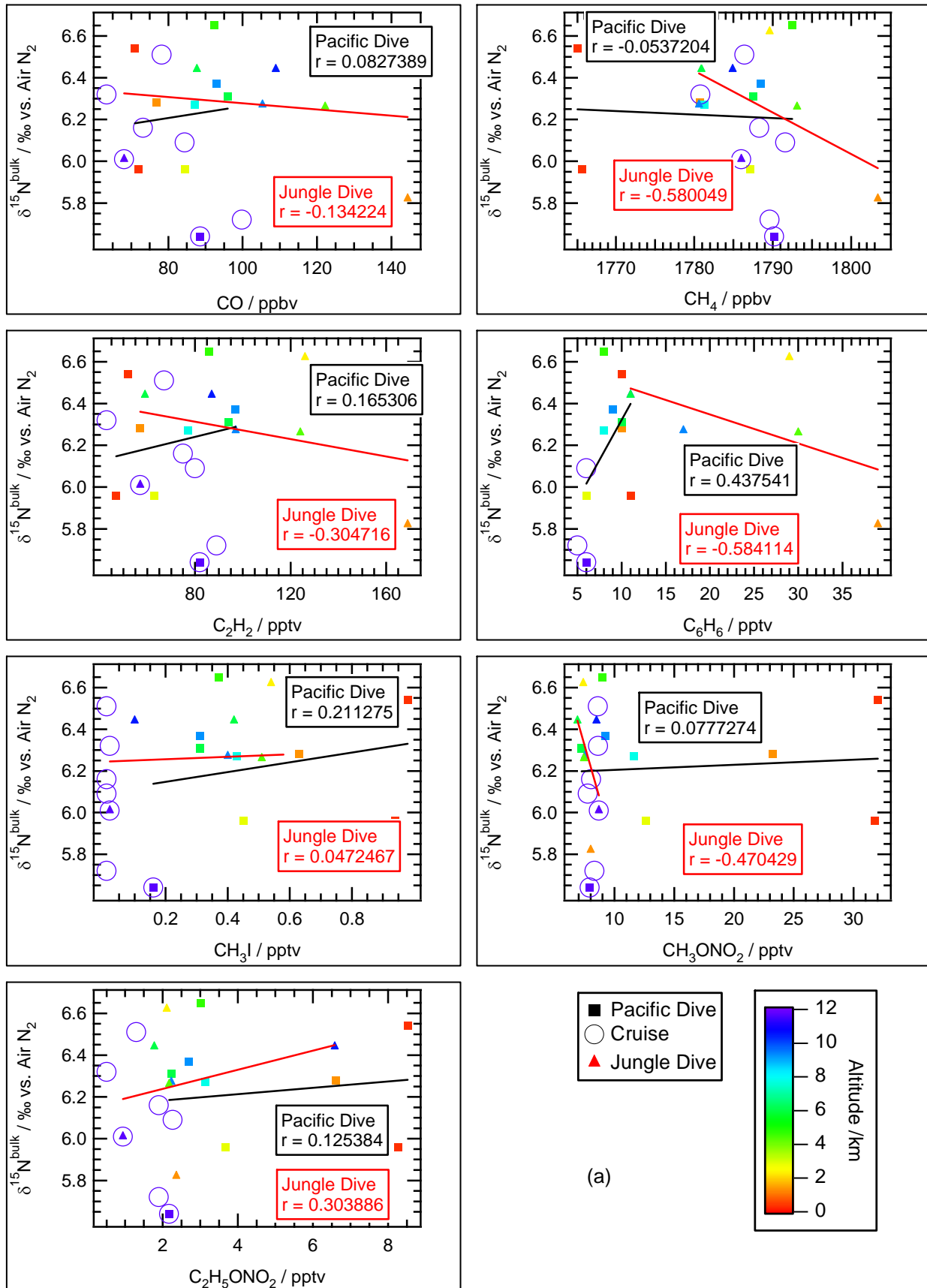


Figure S2:

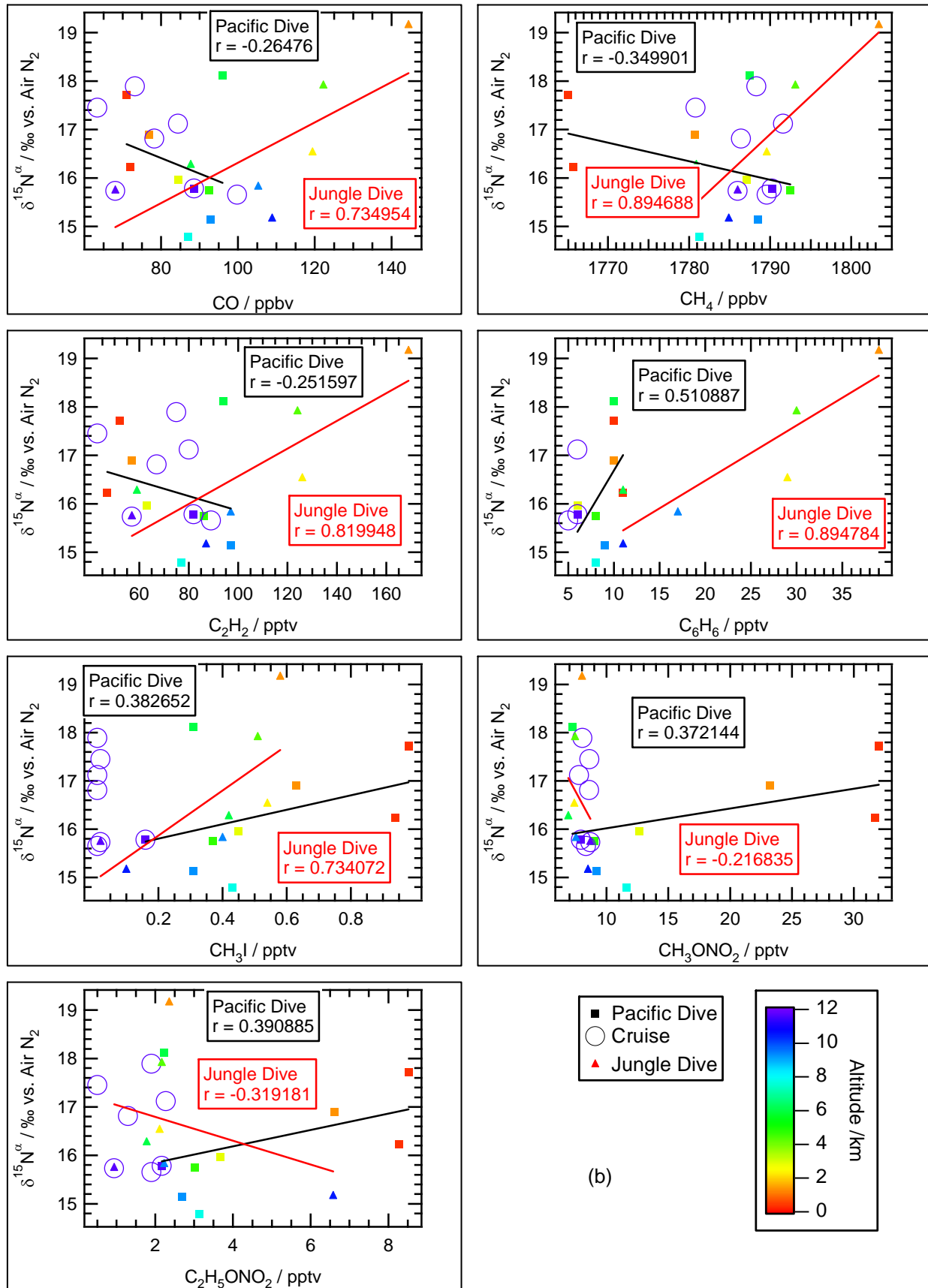


Figure S3:

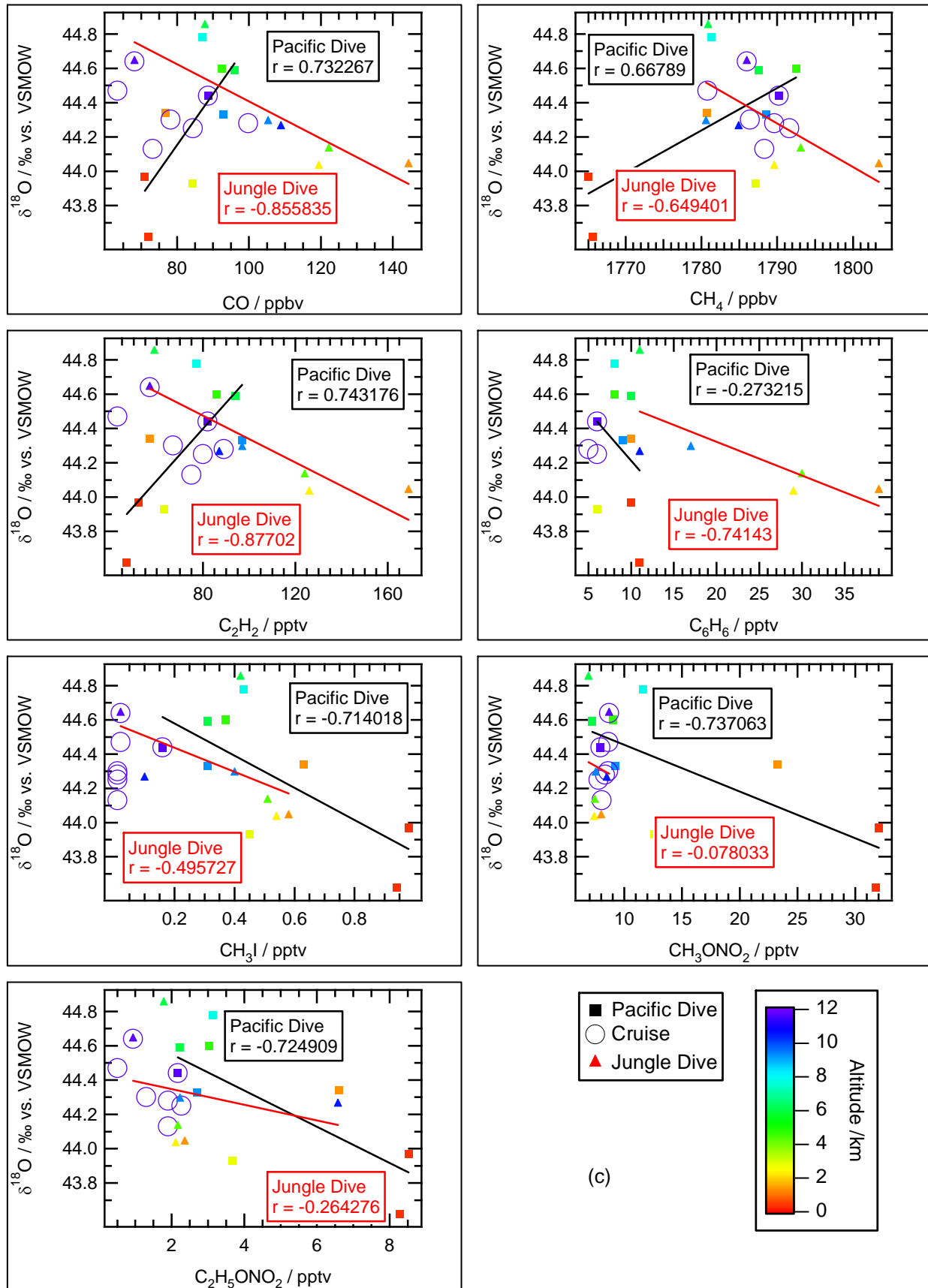


Table S1: N₂O mixing ratio and isotopic composition for the CRAVE WB-57 samples

Flight Date	Time	[N ₂ O] / ppb	$\delta^{15}\text{N}^{\text{bulk}}$ / ‰	$\delta^{18}\text{O}$ / ‰	$\delta^{15}\text{N}^{\alpha}$ / ‰	$\delta^{15}\text{N}^{\beta}$ / ‰	Altitude / km	Latitude / °N	Longitude / °W
20060119	19:18	317.7	6.34	44.13	16.55	-3.68	17.0	-1.1	82.1
20060119	19:22	319.3	6.60	44.25	15.50	-2.10	17.0	-0.8	82.0
20060119	19:23	318.2	6.31	44.68	15.84	-3.02	17.0	-0.7	82.0
20060119	19:27	318.1	6.16	44.81	16.83	-4.34	17.5	-0.3	82.1
20060119	19:30	317.2	6.45	44.53	14.47	-1.33	17.9	0.1	82.1
20060119	19:34	315.8	6.39	44.64	15.76	-2.79	18.2	0.5	82.2
20060119	19:42	315.6	6.46	44.63	15.69	-2.57	18.5	1.3	82.4
20060119	19:49	311.5	6.51	44.10	17.79	-4.61	18.8	2.2	82.5
20060121	17:18	319.1	6.54	44.48	17.48	-4.25	16.9	9.9	81.5
20060121	20:14	312.8	6.72	44.36	16.14	-2.50	19.3	9.9	82.2
20060127	18:01	319.9	5.98	44.09	14.97	-2.81	15.5	4.5	77.6
20060127	18:24	320.4	6.28	44.09	15.85	-3.09	14.7	6.0	79.2
20060127	20:24	319.9	6.11	44.79	15.96	-3.55	8.1	10.0	84.2
20060130	18:04	320.4	6.03	44.63	16.03	-3.79	13.4	8.3	78.3
20060130	19:41	320.0	6.26	44.00	16.43	-3.73	11.9	10.0	84.3
20060130	20:00	318.1	6.33	44.04	15.74	-2.88	2.1	9.9	84.5
20060202	19:54	317.3	6.14	43.99	16.31	-3.85	18.3	3.8	86.0
20060207	17:38	317.0	5.98	43.99	17.08	-4.97	17.8	1.3	81.1
20060207	17:46	318.2	6.27	44.44	16.09	-3.36	17.7	0.4	80.9
20060207	17:53	317.9	6.16	44.24	16.01	-3.51	17.3	-0.3	80.7
20060207	17:56	317.9	6.43	44.14	16.83	-3.79	16.0	-0.6	80.6
20060207	17:59	319.1	6.16	44.39	15.32	-2.79	14.1	-0.8	80.7
20060207	18:02	319.6	6.08	44.39	14.66	-2.30	12.3	-0.6	80.8
20060207	18:05	319.4	5.84	44.45	15.65	-3.78	11.5	-0.3	80.8
20060207	18:08	319.0	6.09	44.31	15.84	-3.48	11.8	0.0	80.9
20060207	18:11	319.3	6.38	44.20	16.13	-3.17	13.4	0.2	80.9
20060207	18:14	319.7	6.47	43.92	14.26	-1.09	14.5	0.6	81.0
20060207	18:18	318.1	6.34	43.52	15.93	-3.05	16.2	1.0	81.0
20060207	18:21	318.3	6.05	43.96	16.26	-3.99	16.8	1.3	81.1
20060207	18:25	317.7	6.08	44.05	15.54	-3.19	17.3	1.7	81.2
20060207	18:28	318.3	6.02	44.11	16.29	-4.07	17.7	2.1	81.3
20060207	18:32	318.0	6.16	44.41	14.36	-1.82	18.1	2.5	81.3
20060207	18:39	317.1	6.31	44.60	16.92	-4.14	18.7	3.3	81.5
20060207	19:01	315.4	6.50	44.59	16.87	-3.70	18.9	5.7	82.2
20060207	20:03	315.5	6.25	44.05	16.10	-3.41	18.0	9.9	84.3
20060209	19:10	321.4	6.01	44.65	15.42	-3.21	13.0	1.9	80.1
20060211	19:53	316.9	6.33	44.78	16.58	-3.73	17.8	21.2	85.9
20060211	19:57	318.6	5.70	43.91	15.38	-3.78	16.5	21.7	86.1
20060211	20:00	319.3	6.29	44.35	15.62	-2.84	14.4	22.0	86.3
20060211	20:03	319.4	6.32	44.38	14.97	-2.10	12.9	22.2	86.4
20060211	20:06	319.4	6.43	44.42	14.83	-1.75	13.3	22.5	86.5
20060211	20:09	319.2	6.10	43.90	16.21	-3.83	14.6	22.7	86.7
20060211	20:19	319.3	6.29	43.71	15.94	-3.16	16.4	23.3	87.5
20060211	20:33	315.3	6.44	44.22	16.31	-3.25	17.8	24.1	88.7
20060211	20:52	304.4	6.15	45.14	15.80	-3.31	18.5	25.4	90.3
20060211	21:11	310.8	6.50	44.69	16.57	-3.40	18.5	26.6	92.0
20060211	21:20	304.1	6.29	44.52	19.52	-6.82	18.6	27.2	92.6
20060211	21:39	301.9	6.76	45.36	18.66	-4.99	18.7	28.7	94.2

Table S2: N₂O mixing ratio and isotopic composition for the TC⁴ WB-57 samples

Flight Date	Time	[N ₂ O] / ppb	$\delta^{15}\text{N}^{\text{bulk}}$ / ‰	$\delta^{18}\text{O}$ / ‰	$\delta^{15}\text{N}^{\alpha}$ / ‰	$\delta^{15}\text{N}^{\beta}$ / ‰	Altitude / km	Latitude / °N	Longitude / °W
20070803	15:51	309.4	6.93	43.97	17.07	-3.03	18.3	10.0	84.2
20070803	15:53	312.2	6.86	43.86	16.93	-3.04	17.7	9.9	84.1
20070803	15:55	319.0	6.06	44.69	15.57	-3.24	16.2	10.0	84.0
20070803	15:56	319.9	5.74	43.79	15.99	-4.33	15.2	10.1	84.2
20070803	16:01	321.3	5.88	43.60	15.40	-3.45	13.4	9.9	84.2
20070805	15:11	320.8	6.32	44.43	16.19	-3.36	13.6	6.2	80.7
20070805	15:20	320.6	6.22	43.90	16.27	-3.65	14.0	6.4	81.3
20070805	15:23	321.5	5.98	43.55	15.55	-3.40	14.0	6.4	81.1
20070805	15:28	321.4	6.02	43.82	12.98	-0.69	14.0	6.5	80.7
20070805	15:33	320.8	6.32	45.09	18.31	-5.54	14.0	6.5	80.2
20070805	15:47	321.0	6.50	43.96	15.82	-2.62	14.6	6.2	80.4
20070805	15:52	320.9	5.79	44.01	15.13	-3.36	14.7	6.2	81.0
20070805	15:54	320.5	5.87	44.20	17.23	-5.34	15.4	6.2	81.2
20070805	15:56	320.1	6.14	44.58	17.60	-5.18	15.9	6.4	81.4
20070805	15:58	320.2	6.22	43.69	17.56	-4.96	16.3	6.5	81.3
20070805	16:03	319.7	6.16	43.96	16.35	-3.86	16.9	6.3	81.4
20070805	16:09	318.6	6.28	44.41	16.43	-3.68	17.4	6.9	81.7
20070805	16:15	314.8	6.15	44.54	16.41	-3.94	17.8	7.4	82.1
20070805	16:20	311.4	6.17	44.64	15.82	-3.28	18.1	8.0	82.5
20070805	16:35	320.4	6.51	44.41	16.77	-3.58	16.2	9.3	83.5
20070805	16:37	320.7	6.38	44.32	17.84	-4.92	14.9	9.5	83.8
20070805	16:40	320.7	6.28	44.64	13.41	-0.60	13.9	9.6	84.0
20070805	16:43	320.2	5.98	44.36	14.54	-2.36	12.6	9.8	84.2
20070805	16:45	321.1	6.32	44.13	17.19	-4.40	10.2	10.0	84.3
20070806	14:22	315.7	6.86	44.35	15.79	-1.88	17.2	4.5	90.7
20070806	14:27	319.7	5.85	43.56	17.03	-5.18	16.2	4.1	91.1
20070806	14:30	319.9	6.33	44.46	16.16	-3.31	15.8	3.9	91.4
20070806	14:35	319.9	5.74	44.14	15.32	-3.65	16.8	3.5	91.8
20070806	14:40	317.3	6.12	43.97	16.72	-4.30	17.2	3.1	92.2
20070806	14:47	320.6	5.86	44.08	17.59	-5.72	15.8	2.6	91.9
20070806	14:52	320.6	6.45	44.23	17.30	-4.24	14.8	2.3	91.5
20070806	14:56	320.9	6.35	45.06	14.71	-1.79	13.9	2.0	91.1
20070806	14:57	320.9	6.35	44.19	15.54	-2.64	13.7	2.0	91.1
20070806	15:02	320.8	6.38	44.37	16.36	-3.43	14.8	2.1	90.7
20070808	13:37	320.4	5.94	44.56	15.76	-3.70	12.7	5.9	82.4
20070808	13:41	320.4	6.45	44.21	16.29	-3.21	12.1	6.2	82.7
20070808	14:24	320.9	6.03	44.63	16.46	-4.24	11.5	6.7	83.8
20070808	14:28	320.6	6.23	44.45	14.84	-2.15	11.5	6.7	84.2
20070808	14:32	320.9	5.98	44.23	16.12	-3.97	11.7	6.9	84.4
20070809	15:16	315.1	6.50	44.76	17.15	-4.00	16.5	22.0	90.3
20070809	15:23	320.1	5.84	43.68	16.03	-3.32	14.3	22.7	90.7
20070809	15:31	319.1	6.32	44.53	16.07	-3.24	15.8	23.5	91.2
20070809	15:36	314.2	6.11	44.64	16.13	-3.82	16.7	24.0	91.5
20070809	15:51	309.7	6.39	44.26	16.19	-3.46	17.5	25.5	92.4
20070809	16:02	302.4	6.72	45.15	18.35	-4.45	18.3	26.6	93.1
20070809	16:08	295.8	6.54	44.88	14.50	-1.25	18.7	27.2	93.5
20070809	16:13	296.3	7.46	45.16	17.64	-2.80	19.1	27.7	93.8
20070809	16:15	298.7	7.08	45.09	17.97	-3.95	18.6	27.9	93.9
20070809	16:42	317.7	6.50	44.04	18.30	-5.17	1.9	29.4	94.9

Table S3: N₂O isotopic composition for the TC⁴ DC-8 samples

Flight Date	Time	$\delta^{15}\text{N}^{\text{bulk}} /$ ‰	$\delta^{18}\text{O} /$ ‰	$\delta^{15}\text{N}^{\alpha} /$ ‰	$\delta^{15}\text{N}^{\beta} /$ ‰	Altitude / km	Latitude / °N	Longitude / °W
20070805	16:26	6.58	43.76	16.38	-3.02	11.3	6.3	78.5
20070805	16:34	6.00	44.54	16.53	-4.36	9.2	5.7	78.1
20070805	16:39	6.38	44.58	17.74	-4.83	7.8	5.6	77.9
20070805	16:42	6.05	44.42	14.34	-2.02	6.2	5.7	78.1
20070805	16:47	6.21	44.16	16.21	-3.61	4.2	5.5	78.0
20070805	16:53	5.84	44.57	15.81	-3.96	1.5	5.7	78.1
20070805	16:57	6.27	43.64	14.63	-1.88	0.3	5.7	77.9
20070808	16:25	5.96	43.62	16.23	-4.14	0.5	5.2	83.1
20070808	16:31	6.54	43.97	17.72	-4.49	0.5	5.1	82.7
20070808	16:39	6.28	44.34	16.90	-4.17	1.4	5.0	82.1
20070808	16:44	5.96	43.93	15.96	-3.87	2.9	5.0	81.7
20070808	16:48	6.65	44.60	15.75	-2.25	4.7	5.0	81.3
20070808	16:51	6.31	44.59	18.12	-5.35	6.0	5.0	81.0
20070808	16:56	6.27	44.78	14.79	-2.03	7.8	4.6	80.6
20070808	16:59	6.37	44.33	15.14	-2.19	9.2	4.4	80.3
20070808	17:13	5.64	44.44	15.78	-4.32	11.6	4.3	79.1
20070808	17:33	6.09	44.25	17.12	-4.79	11.6	4.9	77.0
20070808	17:43	6.16	44.13	17.89	-5.42	11.6	4.8	75.8
20070808	17:53	5.72	44.28	15.65	-4.02	11.6	4.8	74.8
20070808	18:03	6.51	44.30	16.81	-3.61	11.6	4.2	73.8
20070808	18:13	6.32	44.47	17.45	-4.65	11.6	3.5	72.9
20070808	18:23	6.01	44.64	15.73	-3.53	11.6	3.0	71.9
20070808	18:29	6.44	44.26	15.15	-2.07	10.4	2.7	71.3
20070808	18:31	6.27	44.29	15.81	-3.07	9.3	2.5	71.1
20070808	18:36	6.44	44.85	16.26	-3.18	6.1	2.2	70.8
20070808	18:38	6.26	44.13	17.90	-5.23	4.4	2.0	70.7
20070808	18:40	6.62	44.03	16.52	-3.09	2.4	1.8	70.5
20070808	18:42	5.82	44.04	19.15	-7.41	1.5	1.6	70.5

Table S4: TC⁴ DC-8 mixing ratio data

Flight Date	Time	C ₂ H ₂ / pptv	C ₆ H ₆ / pptv	CH ₃ I / pptv	CH ₃ ONO ₂ / pptv	C ₂ H ₅ ONO ₂ / pptv	CO* / ppbv	CH ₄ * / ppbv
20070805	16:26	144	28	0.26	8.06	5.74	109.3	1806.3
20070805	16:34	177	38	0.22	7.17	4.92	117.8	1805.6
20070805	16:39	71	12	0.26	6.14	2.05	89.2	1787.9
20070805	16:42	60	7	0.16	6.09	1.84	84.0	1773.6
20070805	16:47	106	20	0.46	6.9	2.08	111.5	1795.6
20070805	16:53	124	21	0.6	9.74	3.87	109.2	1801.7
20070805	16:57	120	22	0.66	12.77	4.41	105.0	1800.8
20070808	16:25	47	11	0.94	31.74	8.27	72.0	1765.7
20070808	16:31	52	10	0.98	32.03	8.52	71.0	1765.1
20070808	16:39	57	10	0.63	23.23	6.61	76.8	1780.7
20070808	16:44	63	6	0.45	12.63	3.68	84.4	1787.1
20070808	16:48	86	8	0.37	9.00	3.02	92.4	1792.5
20070808	16:51	94	10	0.31	7.24	2.23	96.0	1787.5
20070808	16:56	77	8	0.43	11.60	3.14	87.0	1781.3
20070808	16:59	97	9	0.31	9.21	2.69	92.9	1788.5
20070808	17:13	82	6	0.16	7.93	2.17	88.6	1790.2
20070808	17:33	80	6	0.01	7.77	2.27	84.4	1791.6
20070808	17:43	75	-	0.01	8.04	1.90	73.2	1788.3
20070808	17:53	89	5	0.01	8.33	1.90	99.8	1789.6
20070808	18:03	67	-	0.01	8.60	1.30	78.2	1786.4
20070808	18:13	43	-	0.02	8.62	0.51	63.4	1780.8
20070808	18:23	57	-	0.02	8.69	0.94	68.1	1786.0
20070808	18:29	87	11	0.10	8.49	6.58	108.9	1784.9
20070808	18:31	97	17	0.40	7.53	2.23	105.3	1780.6
20070808	18:36	59	11	0.42	6.90	1.78	87.7	1780.9
20070808	18:38	124	30	0.51	7.44	2.17	122.2	1793.1
20070808	18:40	126	29	0.54	7.39	2.11	119.4	1789.6
20070808	18:42	169	39	0.58	8.00	2.36	144.4	1803.4

* Mixing ratios are the average of the *in situ* measurements of CO and CH₄ over the DC-8 canister filling times.